

Contents lists available at ScienceDirect

Solar Energy

journal homepage: www.elsevier.com/locate/solener





Low temperature heating operation performance of a domestic heating system based on indirect expansion solar assisted air source heat pump

Li Wei Yang ^a, Yan Li ^b, Tong Yang ^c, Hua Sheng Wang ^{a,*}

- a School of Engineering and Materials Science, Queen Mary University of London, Mile End Road, London E1 4NS, UK
- ^b Gemological Institute, China University of Geosciences, Wuhan, Hubei 430074, China
- ^c Faculty of Science and Technology, Middlesex University, London NW4 4BT, UK

ARTICLE INFO

Keywords:

Low temperature heating Solar assisted air source heat pump Domestic heating Seasonal performance factor Numerical simulation

ABSTRACT

Reducing electricity consumption is of great importance by improving the operation performance of the heating systems based on solar-assisted air source heat pumps for domestic heating. The set hot-water-supply temperature of the heating system affect both the system operation performance and the indoor thermal comfort condition. The effect of low temperature heating on the system operation performance is investigated to figure out the way to significantly save electricity. A single-family house is chosen as the reference building and the heating system is modelled and simulated under the weather conditions in the locations of London, Aughton and Aberdeen in the UK over a year. The set hot-water-supply temperatures are taken to be 40 $^{\circ}$ C, 45 $^{\circ}$ C, 50 $^{\circ}$ C and 55 $^{\circ}$ C. For the heating systems, with the decrease in set hot-water-supply temperature from 55 $^{\circ}$ C to 40 $^{\circ}$ C, the yearly seasonal performance factor increases by 16.7%, 19.1% and 15.4% in London, Aughton and Aberdeen, respectively. Consequently, the yearly total electricity consumption decreases by 19.1%, 14.9% and 13.3% in London, Aughton and Aberdeen, respectively. The results show that low temperature heating enables significant reduction in electricity consumption of such heating systems.

1. Introduction

In the UK, decarbonisation in domestic heating is an important approach to achieve the goal for net-zero emissions of greenhouse gases by 2050 (Committee on Climate Change, 2020). The operation performance of domestic heating systems can be affected by many factors, such as weather conditions, system scale and hot water supply temperature. According to the reports of the International Energy Agency, district heating is transforming from high-temperature heat distribution (3rd generation, above 70 °C) to low-temperature heat distribution (4th generation, 50-70 °C) and ultra-low-temperature district heating (5th generation, below 50 °C) (International Energy Agency, 2021). The transition to low temperature district heating can bring reductions in heat loss by 25 % (Nord et al., 2018) and cost by 10 % (Schmidt et al., 2021). Golmohamadi and Larsen (Golmohamadi and Larsen, 2022) proposed a controller for low temperature district heating via the on/off control of domestic radiator valves and the mass flow rate control of valves in the mixing loop connected to the district heating network. This controller can respond to dynamic electricity price and benefit to adopt intermittent renewable energy into district heating.

Some studies used booster heat pumps (HPs) to elevate the hot water temperature from the low temperature of the district heating to the temperature required for end users (Hesaraki et al., 2015). Yang et al. (Yang et al., 2016) simulated water thermal energy storage (TES) tank and heat pump systems for low temperature district heating and found that the micro heat pump has higher exergy efficiency. Reiners et al. (Reiners et al., 2021) experimentally studied the booster HP with low temperature heating. The results showed that the efficiency of the booster HP is twice of that of ground source heat pump. Quirosa et al. (Quirosa et al., 2022) numerically simulated two types of CO2 booster HPs connected to low temperature district heating network for space heating and hot water. They suggested that the booster heat pump with decoupled production better suits high heat demand. Zhu et al. (Zhu et al., 2021) reported experiments on steady-state behaviour of the booster HP for hot water in low temperature district heating network. The booster HP enables a coefficient of performance (COP) of 4.95 when the water temperatures at the inlets of both condenser and evaporator are 45 °C (water temperature of the district heating) and the condensing temperature is 60 °C.

For individual buildings, the feasibility of low temperature space heating has been analysed and confirmed by Kilkis (Kilkis, 2021). Sarbu

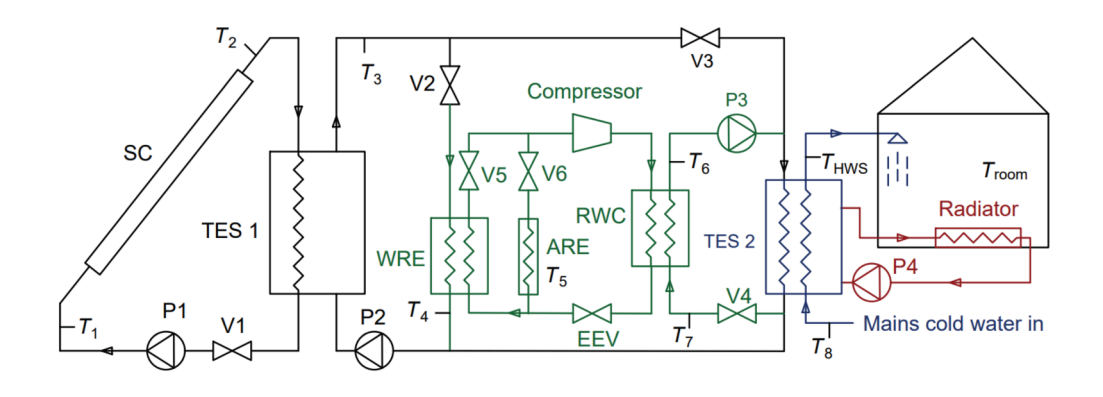
^{*} Corresponding author at: School of Engineering and Materials Science, Queen Mary University of London, Mile End Road, London E1 4NS, UK. E-mail address: h.s.wang@qmul.ac.uk (H.S. Wang).

| Nomenclature $C_{\rm i}$ initial cost difference, GBP $C_{\rm i0}$ initial cost of the studied system, GBP $C_{\rm ieh}$ initial cost of the electrical water heater, GBP $C_{\rm o0}$ operation cost of the studied system, GBP $C_{\rm oeh}$ operation cost of the electrical water heater, GBP COP coefficient of performance $C_{\rm spy}$ cost saving per year, GBP | T_{room} room air temperature, °C T_{HWS} hot-water-supply temperature (hot water temperature at the outlet of TES tank 2), °C T_{HWS}^* set hot-water-supply temperature, °C W_{ASHP} electricity consumed by the air source heat pump, MWh W_{Pump} electricity consumed by a heat pump, MWh W_{SWHP} electricity consumed by all the pumps, MWh W_{SWHP} electricity consumed by the solar water heat pump, MWh W_{tot} total electricity consumed, MWh |
|---|--|
| P_{pb} payback period, year Q_{ASHP, con} thermal energy obtained at the condenser of air source heat pump, MWh Q_{HP,con} thermal energy obtained at the condenser of a heat pump, MWh Q_{HW} thermal energy for hot water, MWh Q_{SH} thermal energy for space heating, MWh Q_{su} solar energy used, MWh Q_{sup} thermal energy supply, MWh Q_{SWHP, con} thermal energy obtained at the condenser of solar water heat pump, MWh Q_{TES} thermal energy storage, MWh I local solar irradiance for the tilted surface, W/m² SF solar fraction SPF_{HP} seasonal performance factor of the heat pump SPF_{SVS} seasonal performance factor of the system | ASHP air source heat pump HP heat pump HW hot water IX-SAASHP indirect expansion solar-assisted air source heat pump SAASHP solar-assisted air source heat pump |

and Sebarchievici (Sarbu and Sebarchievici, 2015) conducted numerical simulation and site measurements, and recommended radiator heating system for low temperature space heating. Solar energy is a kind of clean energy with great potential of applications (Kong et al., 2020) and can be combined with heating technologies for domestic use (Kong et al., 2018). The combination of solar thermal energy and HP (Ma et al., 2020), solar assisted air source heat pump (SAASHP), is expected to be a

promising technology for a green future (Xian et al., 2020). Chaturvedi et al. (Chaturvedi et al., 2014) numerically simulated a direct expansion SAASHP for low temperature water heating and verified the advantages of SAASHP to be high efficiency and low cost. Fraga et al. (Fraga et al., 2017) pointed out that low space heating distribution temperature benefits to achieve higher seasonal performance factor (SPF) of SAASHP.

The dual-source indirect expansion SAASHP (IX-SAASHP) system



Seven loops in the heating system:

(1) Solar collection loop: SC-TES1-V1-PA-SC

(2) TES1-WRE loop: TES1-V2-WRE-P2-TES1

(3) ASHP loop: ARE-V6-Compressor-RWC-EEV-ARE

(4) space heating loop: TES2-Radiator-P4-TES2

(5) TES1-TES2 loop: TES1-V3-TES2-P2-TES1

5) 1231 1232 100p. 1231-13-1232-12-1231

(6) RWC-TES2 loop: RWC-P3-TES2-V4-RWC

(7) SWHP loop: WRE-V5-Compressor-RWC-EEV-WRE

SC: Solar collector

TES 1, TES 2: TES tank

V1 - V6: Valve

P1 - P4: Water pump

WRE: Water-to-refrigerant evaporator ARE: Air-to-refrigerant evaporator RWC: Refrigerant-to-water condenser

EEV: Expansion valve $T_1 - T_8$: temperature sensor

Fig. 1. Schematic and control flow chart of the heating system.

makes use of both solar thermal energy collected by solar collectors and thermal energy extracted from ambient air as the low temperature heat sources for the evaporator(s) of the HP unit (Ran et al., 2020). Though in previous studies, the *COP*s of most dual-source IX-SAASHPs were lower than 3.5 (Yang et al., 2021), the simulation results of Yang et al. (Yang et al., 2022) showed that, the dual-source IX-SAASHP can satisfy the heating demands under the UK weather conditions with a yearly *SPF* of 4.4. Therefore, the dual-source IX-SAASHP is a competitive choice for domestic heating in the UK.

Earlier studies investigated district heating with low temperature and showed higher operation performance and lower energy consumption. So far, few studies have been done for low temperature heating and its effect on the operation performance of IX-SAASHP based domestic heating systems. The present work aims at analysing the low temperature heating of SAASHP heating system for a SFH 45 building in different locations of London (51.5° N), Aughton (53.5° N) and Aberdeen (57.5° N) in the UK. The set hot-water-supply temperature for hot water and space heating varies from 55 °C to 40 °C. A dual-source IX-SAASHP based heating system is employed for heat provision for space heating and hot water at a rate of 300 L/day over a typical meteorological year. The dynamic performance of the heating system is modelled and simulated using TRNSYS 17. Its *COP* and *SPF* are evaluated. The technoeconomic analyses are performed based on the energy prices in the UK.

2. Dual-source indirect expansion solar assisted air source heat pump

The heating system and its performance evaluation are briefly described below. The heating system is used to evaluate the application performance of low temperature heating for SFH 45 in London, Aughton and Aberdeen.

2.1. Description of the heating system

The model of the dual-source IX-SAASHP is established in TRNSYS 17. Water is adopted as the heat transfer and thermal energy storage medium. Two water tanks serve for TES: the outdoor tank stores thermal energy collected by the solar collector and the indoor tank stores thermal energy for demand side – space heating and/or hot water. This work investigates the operation performances of the dual-source IX-SAASHP with different set hot-water-supply temperatures ($T_{\rm HWS}^*$). In the TRNSYS model, a solar water heat pump (SWHP) module and an air source heat pump (ASHP) module together represent a dual-source heat pump unit. Refrigerants R134a and R410A are used as the working fluid for both SWHP and ASHP modules.

Fig. 1 shows the schematic of the heating system. It consists of seven loops including a solar energy collection loop (black), a SWHP-ASHP unit (green), a hot water loop (blue) and a space heating loop (red). The solar collector extracts solar energy and heats up water which is stored in the TES tank 1. The hot water in TES tank 1 can be circulated by pump 2 to TES tank 2 if water temperature in TES tank 1 is higher. The SWHP-ASHP unit includes a water-to-refrigerant evaporator, an air-torefrigerant evaporator, a refrigerant-to-water condenser, a compressor, and an expansion valve. When the unit operates in SWHP mode, the TES tank 1 works as the low temperature heat source and the TES tank 2 works as the high temperature heat source. When the unit operates in ASHP mode, the outdoor air works as the low temperature heat source. When the heating system serves for hot water, the mains cold water flows in a heat exchanger inside the TES tank 2 and is heated to a required temperature. When the heating system serves for space heating, pump 4 circulates the hot water in TES tank 2 to the radiators. The indoor air temperature (T_{room}), outdoor air temperature (T_{amb}), local solar irradiance for the tilted surface (I) and water temperatures at some specific locations, e.g., the inlet and outlet of the solar collector (T_1, T_2) , the outlet of TES tank 1 to load (T_3) and TES tank 2 (hot-water-supply temperature, T_{HWS}), are measured and monitored. The water and air

Table 1TRNSYS module for modelling the temperatures of house ground in London, Aughton and Aberdeen.

| Parameter | Value London | Aughton | Aberdeen |
|--------------------------------------|-----------------|-----------|-----------|
| Mean surface Temperature, °C | 10.78 | 10.04 | 7.84 |
| Amplitude of surface temperature, °C | 18.04 | 14.61 | 16.17 |
| Time shift | 12th day | 359th day | 359th day |

temperatures at the outlet of the evaporators (T_4 and T_5), the water temperatures at the inlet and outlet of the condenser (T_6 and T_7) and the temperature of the mains water supply (T_8) are measured/monitored. These temperatures are used for the operation control of the heating system and analysis of the energy conversion. The details of the system operation control are given in a rule-based look-up table in (Yang et al., 2022).

2.2. Evaluation of performance

The indoor air temperature, $T_{\rm HWS}$, SPF of the system ($SPF_{\rm sys}$), SPF of the HP ($SPF_{\rm HP}$), COP of the HP module, and the solar fraction (SF) are used to evaluate the heating system performance.

$$SPF \text{sys} = \frac{\int (Q_{\text{SH}} + Q_{\text{HW}}) \times dt}{\int W_{\text{tot}} \times dt}$$
 (1)

where $Q_{\rm SH}$ is the heat provided for space heating, $Q_{\rm HW}$ is the heat provided for hot water, and $W_{\rm tot}$ is the total electricity consumption given by Eq. (2):

$$W_{tot} = W_{HP} + W_{pump} \tag{2}$$

where W_{pump} is the electricity consumption of all water pumps, W_{HP} is the electricity consumption of the HP unit given by Eq. (3):

$$W_{HP} = j_{ASHP} W_{ASHP} + j_{SWHP} W_{SWHP}$$
(3)

where $W_{\rm ASHP}$ and $W_{\rm SWHP}$ are the electricity consumed in the ASHP mode and SWHP mode, respectively, $j_{\rm ASHP}$ and $j_{\rm SWHP}$ have values either 1 or 0 representing on/off status of the ASHP mode and SWHP mode.

$$SPFHP = \frac{\int Q_{HP, con} \times dt}{\int W_{HP} \times dt}$$
 (4)

where $Q_{\rm HP,con}$ is the heat transferred from the condenser to the TES tank 2 in the corresponding HP mode, calculated by Eq. (5):

$$Q_{HP,con} = j_{ASHP}Q_{ASHP,con} + j_{SWHP}Q_{SWHP,con}$$
(5)

where QASHP, con and QSWHP, con are the values of heat transferred

Table 2
Weather conditions in London, Aughton and Aberdeen during the heating season.

| | | London | Aughton | Aberdeen |
|-----------------------------|---------------|---------|---------|----------|
| Latitude | | 51.5° N | 53.5° N | 57.5° N |
| Average sky cover rate (Day | rtime) | 81.32 % | 77.32 % | 75.83 % |
| Ambient temperature (°C) | Min | -3 | -3.95 | -6.7 |
| | Max | 18.3 | 16 | 16.8 |
| | Average | 6.61 | 7.42 | 5.64 |
| Solar radiation intensity | Min (Daytime) | 0.96 | 0.94 | 0.93 |
| (W/m^2) | Max | 1115.73 | 1101.98 | 1113.9 |
| | Average | 199.3 | 229.2 | 233.8 |
| | (Daytime) | | | |
| Wind speed (m/s) | Min | 0.1 | 0.15 | 0.1 |
| | Max | 14.1 | 23.51 | 16.1 |
| | Average | 4.23 | 5.82 | 4.99 |

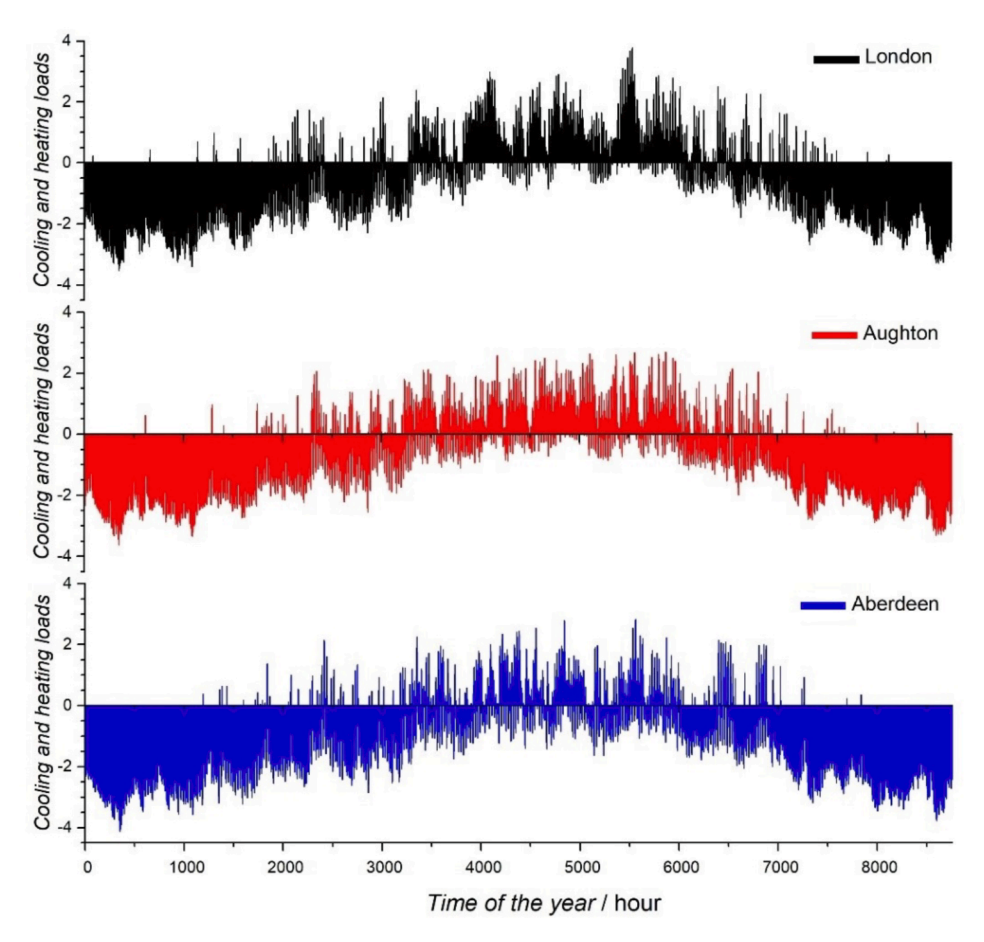


Fig. 2. Hourly cooling (positive) and heating (negative) loads of the house SFH 45 at room air temperature $T_{\rm room}$ of 20 °C over a typical year of weather conditions in London, Aughton and Aberdeen.

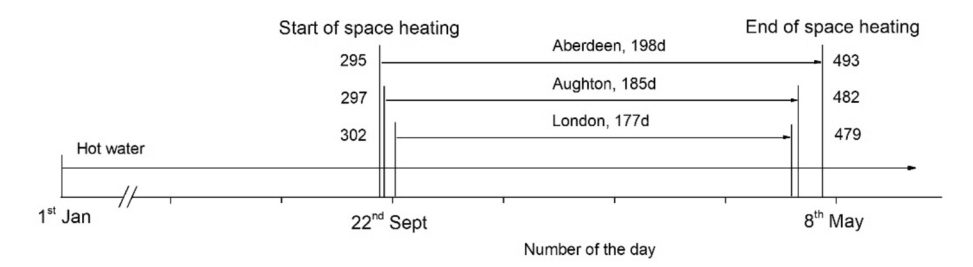


Fig. 3. Schematic of the heating periods for the heating systems under the weather conditions in London, Aughton and Aberdeen.

from the condenser to the TES tank 2 in the ASHP mode and SWHP mode, respectively.

$$COP = Q_{HP,con}/W_{HP} \tag{6}$$

The SF is calculated by Eq.(7):

$$SF = 1 - \frac{\int (Q_{\text{ASHP, con}} + W_{\text{SWHP}}) \times dt}{\int (Q_{\text{HW}} + Q_{\text{SH}}) \times dt}$$
(7)

3. Working conditions

The heating system works for space heating and hot water for a single-family house (SFH) 45 building (Dott et al., 2013). The working conditions including heat demand and operation temperatures are briefly introduced in this section.

3.1. Reference building and heat demand

The standard SFH 45 building of 140 m² is used as the reference building. The geometry, dimensions and other parameters are introduced in (Dott et al., 2013). The ground temperature module in TRNSYS, Type 501, is used to simulate temperature of the building ground at the depth of 0.445 m. Table 1 lists the parameters for model of ground temperatures. Table 2 lists the weather conditions during the heating season. The collector inclination angle at each location is set to be equal to the latitude for maximising solar energy reaching to the collector surface. It is noticed that though Aberdeen has the lowest sky cover rate and highest average solar irradiation intensity (daytime), Aberdeen has the shortest day time due to the highest latitude. Overall, Aughton has the highest solar energy availability, followed by London and Aberdeen. Fig. 2 displays the hourly cooling (positive) and heating (negative) loads of the house SFH 45 at the room air temperature $T_{\rm room}$ of 20 °C over a typical year of weather conditions in London, Aughton and Aberdeen.

Table 3Summary of TRNSYS modules chosen for modelling the components of the heating system and main parameters.

| Component | Module | Parameter | Value |
|-------------------|----------|-----------------------|--|
| Solar collector | Type 1b | Area | 18 m ² |
| | ** | Intercept efficiency | 0.8 |
| | | Efficiency slope | 13 kJ/hm²k |
| | | Efficiency curvature | 0 kJ/hm ² k ² |
| TES tank 1 | Type 4a | Heat loss coefficient | $0.2 \text{ W/(m}^2 \text{ K)}$ |
| | | Volume | 500 L |
| | | Height | 1.175 m |
| TES tank 2 | Type 4a | Heat loss coefficient | $0.2 \text{ W/(m}^2 \text{ K)}$ |
| | ** | Volume | 300 L |
| | | Height | 1 m |
| ASHP | Type 941 | Blower power | 0.15 kW |
| | | Total air flow rate | 1500 L/s |
| | | User defined file | YVAS012, York, Jonson Control |
| SWHP | Type 668 | User defined file | 30HXC-HP2, Carrier United Technologies |
| Pump 1 | Type 110 | Rated flow rate | 500 kg/h |
| • | ** | Rated power | 30 W |
| Pump 2 | Type 110 | Rated flow rate | 800 kg/h |
| _ | | Rated power | 50 W |
| Pump 4 | Type 110 | Rated flow rate | 800 kg/h |
| • | ** | Rated power | 50 W |
| Pump in SWHP loop | Type 110 | Rated flow rate | 870 kg/h |
| - * | ** | Rated power | 50 W |
| Pump in ASHP loop | Type 110 | Rated flow rate | 870 kg/h |
| • | 7.1 | Rated power | 50 W |

The peak heating loads are 3.53 kW, 3.63 kW and 4.15 kW while the average heating loads are 1.76 kW, 1.73 kW and 2.03 kW in London, Aughton and Aberdeen, respectively. The peak heating load in London is seen to be similar to that in Aughton whereas the heating load in Aughton shows less variation than that in London. In Aberdeen, the heating load is generally higher than those in London and Aughton.

For the SFH 45 building, the space heating period is recommended to be the days when the average outdoor air temperature for 24 h is under 14 $^{\circ}$ C. Fig. 3 shows the schematic of the heating periods for the heating systems under the weather conditions in London, Aughton and Aberdeen. For convenience, the heating season is set to be from 1st October to 30th April in the further comparisons. The rest period in the year is the non-heating season.

3.2. Set operation temperatures

The heating system works to supply heat for space heating and hot water for the SFH 45 building over a year in London, Aughton and $\frac{1}{2}$

Aberdeen. The thermal comfort requires the indoor air temperature $T_{\rm room}$ to be 20 \pm 2 °C in the heating season. When the HP modules operate, $T_{\rm HWS}^*$ are set to be 40 °C, 45 °C, 50 °C and 55 °C to investigate the operation performance. Daily hot water consumption is assumed to be four 15-minute water draws of 300 kg/h at 6 am, 8 am, 8 pm and 10 pm. The hot water from TES tank 2 is mixed with mains cold water to a temperature of 40 °C for use (Charted Institute of Plumbing and Heating Engineering). When the heating system works in the solar hot water (SHW) mode, $T_{\rm HWS}^*$ is set to be within 80 °C to ensure the safe operation of the system.

4. Modelling and simulation methods

The simulation is conducted over a year and the time step is set at 1 min. The calculation begins to operate at the 4380 h of the year (the middle point). The initial water temperature in TES tanks is 13.4 $^{\circ}\text{C}$, equal to the temperature of the mains cold water at that time.

The flat pale solar collector module, Type 1b, is adopted in the

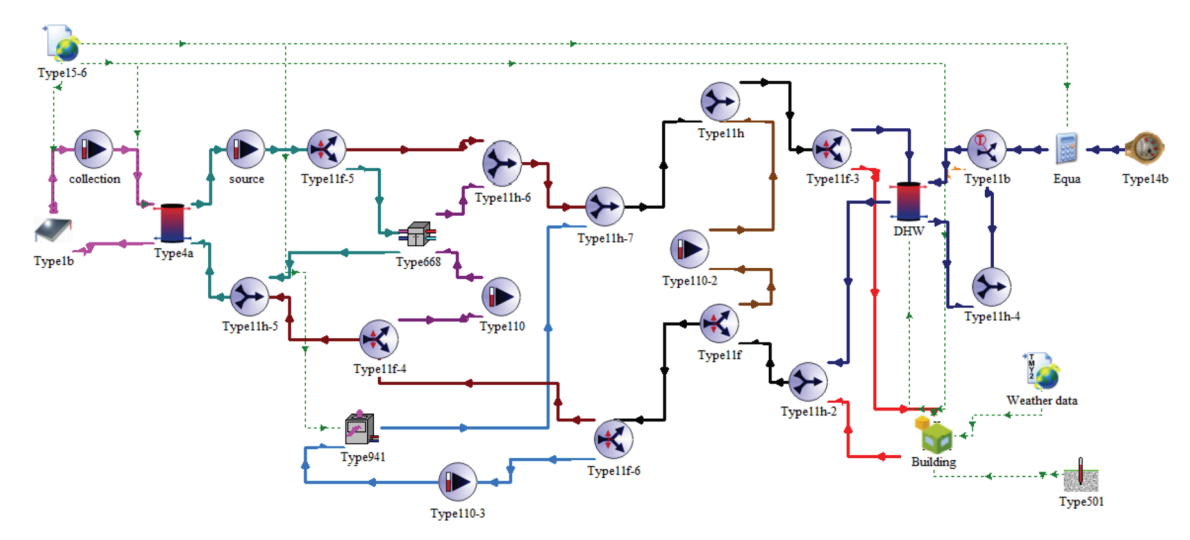


Fig. 4. Models and control functions of the heating system in TRNSYS.

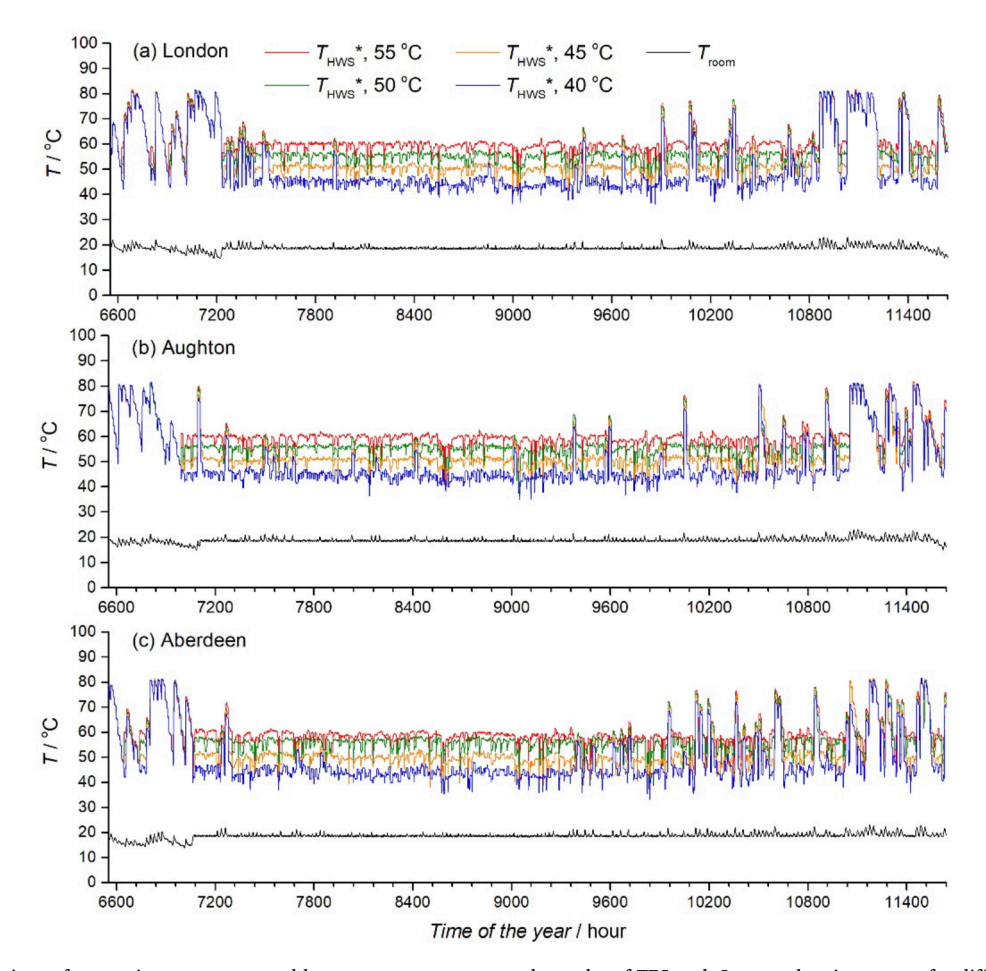


Fig. 5. Variations of room air temperature and hot water temperature at the outlet of TES tank 2 over a heating season for different $T_{\rm HWS}^{\star}$.

TRNSYS model because this kind of solar collector takes around 50 % of the market share (Ruschenburg et al., 2013). To analyse the operation performance of the heating system for different $T_{\rm HWS}^*$, auxiliary heater is not employed. All the heat demands are met by the thermal energy from HPs and direct SHW. When the heat provision is not enough, the indoor air temperature and $T_{\rm HWS}$ drop down below their set values.

The system size is determined according to the heat demands. The solar collector area and TES tank 1 volume are 18 m² and 500 L, respectively. This system scale can ensure $T_{\rm HWS}$ no less than 40 °C in most days of non-heating seasons. If $T_{\rm HWS}$ drops below the set temperature in non-heating seasons, the HPs work to elevate $T_{\rm HWS}$ to the set range.

The dual-source HP is modelled by both a SWHP module, Type 668, and an ASHP module, Type 941. For the purpose of comparison, the heating capacity of the heating system is designed to be 8 kW, same in the three locations. The SWHP module is user defined according to the sample file of 30HXC-HP2 from Carrier United Technologies. The ASHP module is user defined according to the sample file of YVAS012, York, Jonson Control. It should be noted that the ASHP module does not concern the influence of frosting and defrosting on the operation performance of ASHP. The simulation results could describe the right trend of operation performance for different T_{HWS}^* . The TRNSYS modules adopted in the heating system and the corresponding parameters are given in Table 3. The parameters that define the models of the components are derived from the experimental data of the component products available in the market. The system and control functions for the heating system in TRNSYS are shown in Fig. 4. The pipe connections are displayed by the solid lines and the control connections are displayed by the dashed lines.

5. Results and discussions

The heating system is modelled in TRNSYS for the weather conditions in London, Aughton and Aberdeen. Simulations with different $T_{\rm HWS}^*$ are conducted to obtain the operation performance.

5.1. Seasonally heating performance for different T_{HWS}^*

Fig. 5 displays the variations of the room air temperature (black) and hot water temperature at the outlet of TES tank 2 ($T_{\rm HWS}$) over a heating season for different $T_{\rm HWS}^*$. When $T_{\rm HWS}$ drops down below $T_{\rm HWS}^*$, the heat pump switches on to increase $T_{\rm HWS}$. It is seen that the temperature drops in $T_{\rm HWS}$ occur more frequently for lower $T_{\rm HWS}^*$ due to lower capacity of TES at lower temperature. When $T_{\rm HWS}^*$ is set at 40 °C – 50 °C, in all these three locations, the heating system can provide sufficient thermal energy and maintain $T_{\rm HWS}$ around 5 K higher than $T_{\rm HWS}^*$. This suggests that though the heating demand in Aberdeen is much higher than those in London and Aughton, the heating system with the same heating capacity can provide sufficient heat to meet the heating demand in Aberdeen. However, when $T_{\rm HWS}^*$ is set at 55 °C, the heating system under weather conditions in London and Aughton works well and achieves a $T_{\rm HWS}$ of around 60 °C; in Aberdeen, the heating system can only maintain a $T_{\rm HWS}$ of 57 °C, slightly higher than the set temperature.

Taking the operation performance of the heating system in London, for example, Fig. 6 shows the daily variations of heat provision for space heating (green) and hot water (yellow) over a heating season for different $T_{\rm HWS}^*$. The stacked instantaneous values show the total heat provision. The variation of the heat provision for space heating is seen different for different $T_{\rm HWS}^*$. This is attributed to the influence of thermal energy stored in building structures at different temperatures. When

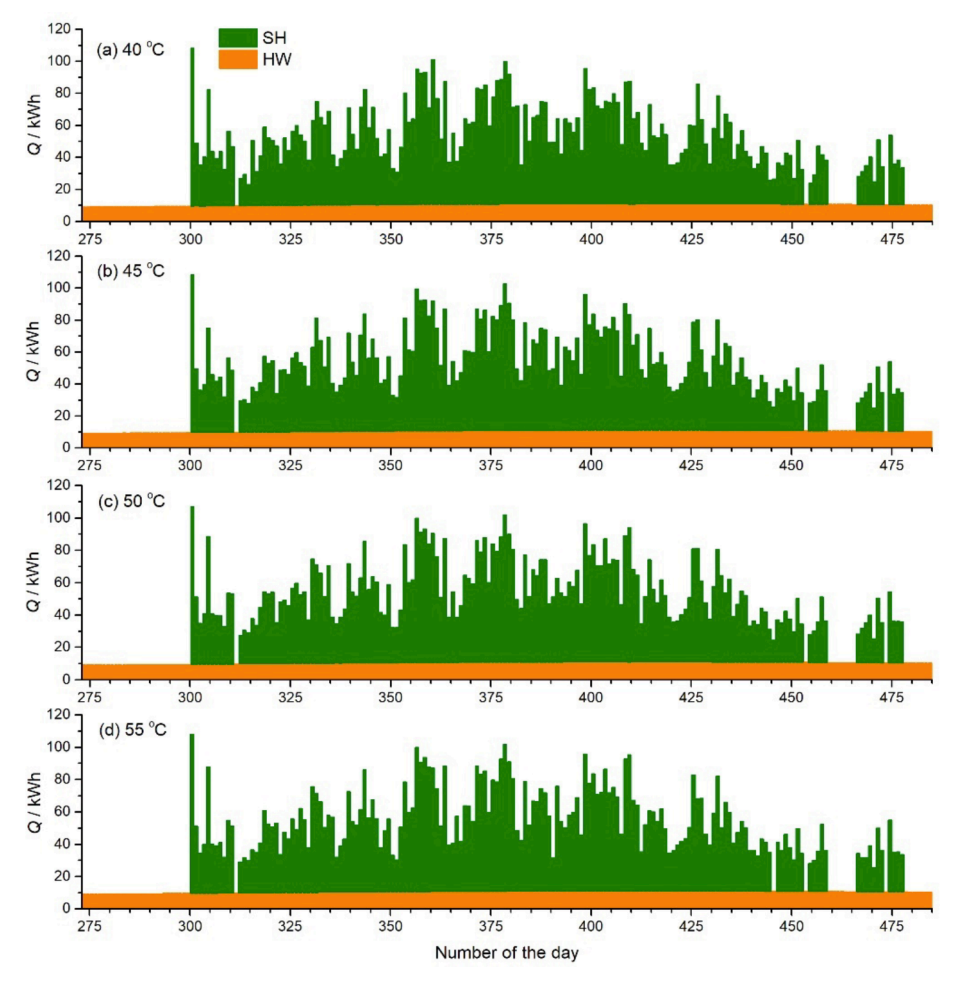


Fig. 6. Daily variations of heat provision for space heating and hot water over a heating season for different T_{HWS}*.

 $T_{\rm HWS}^*$ is set at 40 °C, the heat provision for hot water is slightly lower than the heat demand at the beginning of heating periods (300th day) while at other temperatures of $T_{\rm HWS}^*$, the heat provision meet well with the heat demands. This is because the lower capacity of tank 2 TES at $T_{\rm HWS}^*$ of 40 °C is hardly to meet the sudden increase in heat demand.

Fig. 7 displays the daily variations of heat provision for space heating and hot water by direct SHW, ASHP and SWHP over a heating season for different $T_{\rm HWS}^*$. The red column represents the daily heat provision by ASHP, the yellow column represents that by SWHP, and the purple column represents that by direct SHW. The stacked chart shows the total heat provision. For different $T_{\rm HWS}^*$, the proportions of heat provision contributed by ASHP, SWHP and direct SHW are almost the same and the heat provision by ASHP is dominant. The direct SHW contributes the main heat provision in non-heating period. Additionally, in non-heating period, for example 273th-300th days, the increased contribution of SWHP is observed as $T_{\rm HWS}^*$ increases.

Fig. 8 shows the daily variations of electricity consumed by ASHP (yellow), SWHP (red) and SHW (blue) over a heating season for different $T_{\rm HWS}^*$. Refering to Fig. 7, the electricity is mainly consumed by ASHP. It is also seen that the electricity consumed by SWHP increases as $T_{\rm HWS}^*$ increases in non-heating period. As $T_{\rm HWS}^*$ increases, the electricity consumptions by ASHP and SWHP increase since the condensing temperature increases. For example, on the 381st (16th) day, the total electricity consumptions are 30.9 kWh and 33.5 kWh for $T_{\rm HWS}^*$ of 40 °C and 55 °C, respectively.

Fig. 9 shows the daily variations of thermal energy extracted from solar energy either used as the heat source for SWHP (pink) or directly for hot water (SHW, blue) over a heating season for different $T_{\rm HWS}^*$. The

total solar energy used is almost the same for different $T_{\rm HWS}^*$. As $T_{\rm HWS}^*$ increases, the capacity for direct SHW decreases and therefore more solar thermal energy is used by SWHP. For $T_{\rm HWS}^*$ of 45 °C and above, SWHP is often operated in non-heating periods while in this temperature range, as $T_{\rm HWS}^*$ increases, the total solar energy used by SWHP in nonheating periods remains almost the same.

Fig. 10 shows the daily variations of $Q_{\rm TES}$ charged (positive) and discharged (negative) of tank 2 over a heating season for different $T_{\rm HWS}^*$. Although $T_{\rm HWS}^*$ influences the storage capacity, the daily TES charged and discharged look similar for all different $T_{\rm HWS}^*$.

Fig. 11 shows the variations of daily averaged *COP*s of ASHP and SWHP over a heating season for different $T_{\rm HWS}^*$. For both ASHP and SWHP, *COP* decreases as $T_{\rm HWS}^*$ increases. The variation among $COP_{\rm ASHP}$ for different $T_{\rm HWS}^*$ is relatively small, around 1.0 while the variation among $COP_{\rm SWHP}$ for different $T_{\rm HWS}^*$ is larger, around 2.0. The $COP_{\rm ASHP}$ ranges mainly in 3.0–4.0 while the $COP_{\rm SWHP}$ ranges mainly in 4.0–6.0. On some days such as the 315th day, for both ASHP and SWHP their $COP_{\rm SWHP}$ are apparently higher than those at higher $T_{\rm HWS}^*$.

Fig. 12 shows the daily variations of $SPF_{\rm sys}$ and $SPF_{\rm HP}$ over a heating season for different $T_{\rm HWS}^*$. $SPF_{\rm HP}$ shows the same trend as $COP_{\rm HP}$. The influence of $T_{\rm HWS}^*$ on $SPF_{\rm sys}$ is seen complicated. On most days, low temperature heating achieves better performance, especially in non-heating period. However, on some days such as the 312th day, the trend of the performance is inverse. On some days such as the 479th (114th) day, $SPF_{\rm sys}$ is not influenced by $T_{\rm HWS}^*$: $SPF_{\rm sys}$ decreases as $T_{\rm HWS}^*$ decreases from 55 °C but reaches the highest value at $T_{\rm HWS}^*$ of 40 °C.

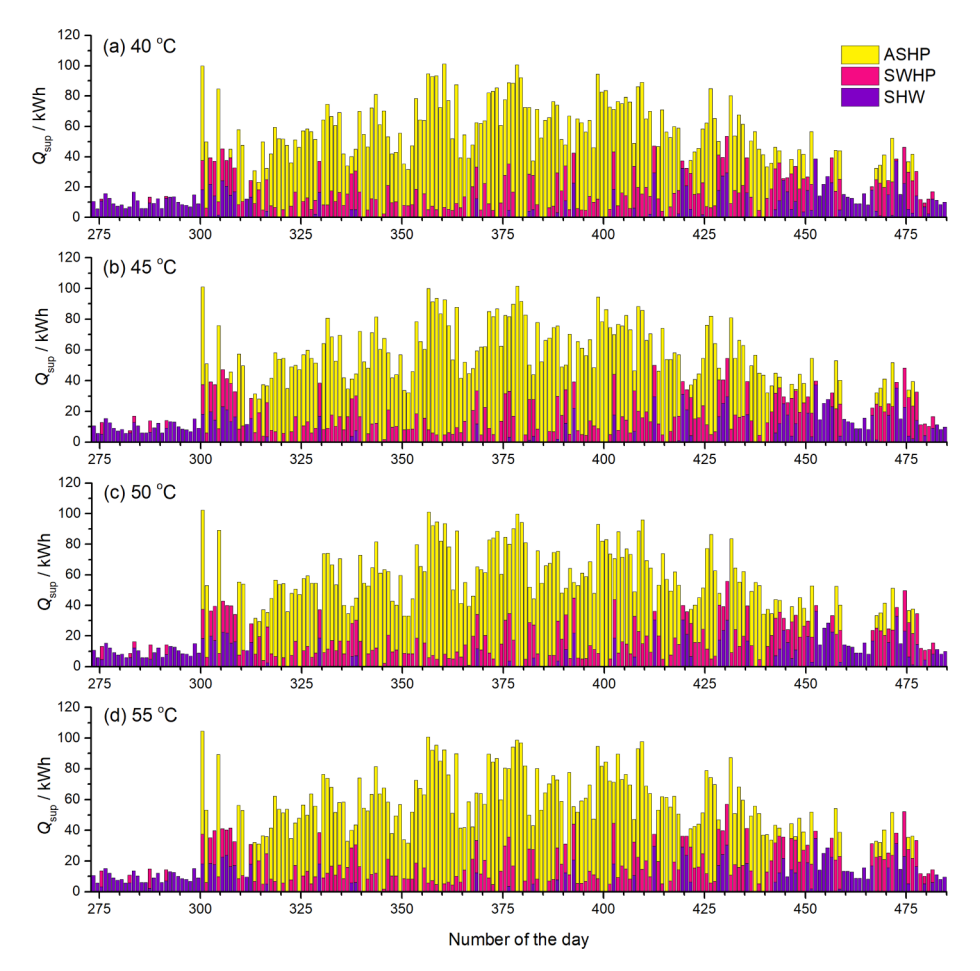


Fig. 7. Daily variations of heat provision for space heating and hot water by direct SHW, ASHP and SWHP over a heating season for different T_{HWS}*.

5.2. Performance of low temperature heating in London, Aughton and Aberdeen

The performances of low temperature heating of the heating system under the weather conditions in London, Aughton and Aberdeen are analysed and compared. Fig. 13 shows the daily variations of heat provision for space heating (green) and hot water (yellow) over a heating season in London, Aughton and Aberdeen, respectively. The heat provision for hot water in Aberdeen is the highest, followed by Aughton and London. This is due to their mains cold water temperatures. The heat provision for space heating shows the same trend to the heating load shown in Fig. 2. In Aberdeen, the daily heat provision for space heating is the highest with large variation and a peak value of 108.4 kWh. In London and Aughton, the daily heat provisions for space heating are relatively lower with the peak values of 90.5 kWh and 90.8 kWh. The heat provision for space heating in Aughton shows less variation.

Fig. 14 shows the daily variations of heat provision for space heating and hot water by direct SHW (purple), ASHP (yellow) and SWHP (red) over a heating season in London, Aughton and Aberdeen, respectively. In the heating season, ASHP, SWHP and direct SHW contribute to 66.3 %, 21.2 % and 12.5 % of the total heat in London, 63.1 %, 24.6 % and 12.3 % in Aughton and 67.3 %, 22.9 % and 9.8 % in Aberdeen, respectively. It is seen that the heat provided by ASHP is about three times of that by SWHP and about six times of that by direct SHW in the three locations. It is also noted that in some days e.g. from 329th to 385th, all the heat is solely supplied by HPs (ASHP 87.6 % and SWHP 12.4 %) in Aberdeen.

Fig. 15 shows the daily variations of electricity consumed by ASHP (yellow), SWHP (red) and pumps (blue) over a heating season in

London, Aughton and Aberdeen, respectively. The electricity consumptions over the heating season in London, Aughton and Aberdeen are 2221.1 kWh, 2246.5 kWh and 3067.0 kWh. In the heating season, the proportions of the electricity consumption by ASHP, SWHP and pumps are 70.9 %, 16.7 % and 12.4 % in London, 68.5 %, 19.1 % and 12.3 % in Aughton and 70.9 %, 17.4 % and 11.6 % in Aberdeen, respectively. It is seen that the electricity consumed by ASHP is about four times of that by SWHP and about five times of that by pumps in the three locations. Though heat is not supplied directly by SHW in the period of 329th – 385th day in Aberdeen, the electricity consumption by water pumps is 146.2 kWh to assist the operation of SWHP and to charge the TES tank 1.

Fig. 16 shows the daily variations of thermal energy extracted from solar energy either used as the heat source for SWHP (pink) or direct solar hot water (SHW, blue) over the heating season in London, Aughton and Aberdeen, respectively. In the heating season, the total solar energy utilized in London, Aughton and Aberdeen is 3.0 MWh, 3.3 MWh and 3.6 MWh, respectively. The proportions of the solar energy utilized by SWHP and direct SHW are 58.2 % and 41.8 % in London, 62.3 % and 37.7 % in Aughton and 65.7 % and 34.3 % in Aberdeen, respectively. It is seen that more solar energy is utilized by SWHP at higher latitude. In some days, e.g. 426th (61st) day, the solar thermal energy extracted in London is only 5.79 kWh while those in Aughton and Aberdeen are 21.9 kWh and 39.3 kWh. Furthermore, in December, the solar thermal energy is seen to provide large direct SHW of 69.8 kWh in Aughton. This is due to the unpredictable weather conditions in these locations.

Fig. 17 shows the daily variations of averaged COP of the HPs over a heating season in London (blue), Aughton (orange) and Aberdeen (green). In all the three locations, the values of COP_{ASHP} fall in the range of 3.0–4.0. The COP_{ASHP} in Aberdeen is slightly lower than those in

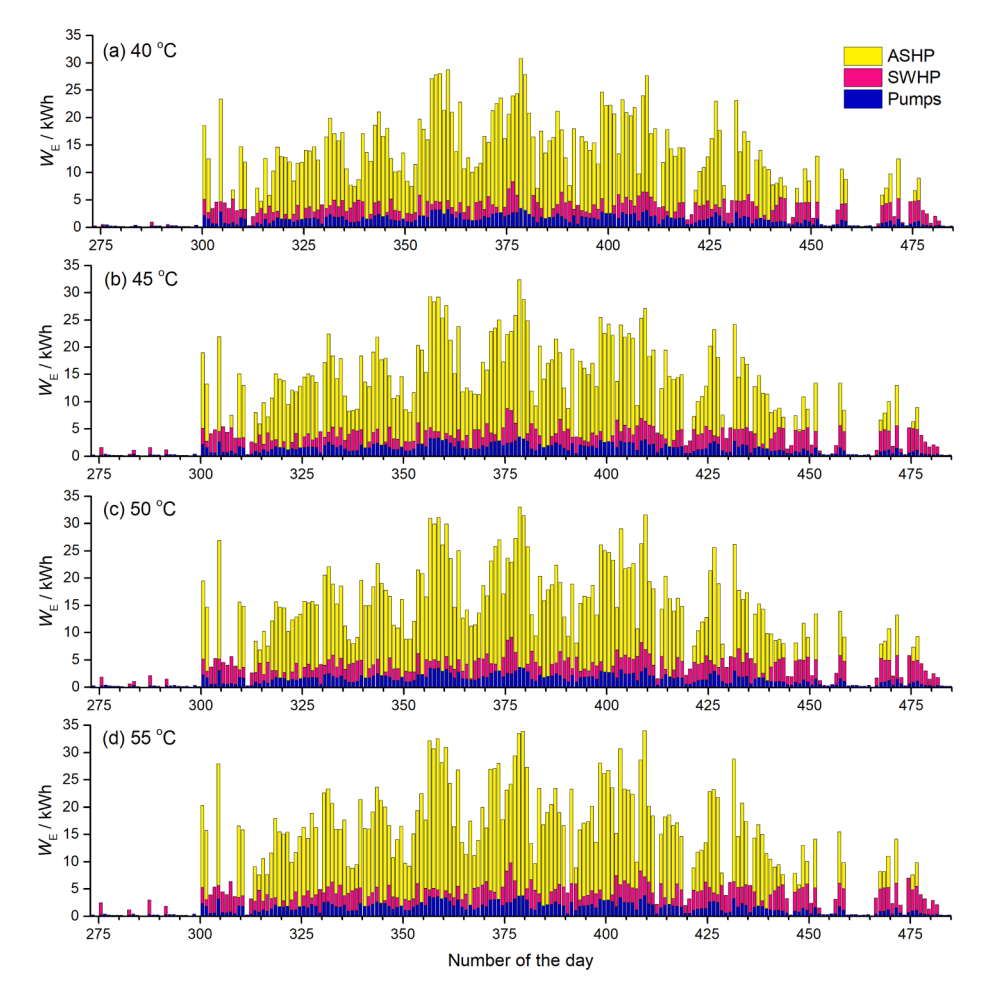


Fig. 8. Daily variations of electricity consumed $W_{\rm E}$ by ASHP, SWHP and SHW over a heating season for different $T_{\rm HWS}^*$.

London and Aughton. The averaged values of COP_{ASHP} are 3.8, 3.8 and 3.6 in London, Aughton and Aberdeen, respectively. In contrast, the values of COP_{SWHP} in the three locations vary largely from 3.0 to 7.0 in autumn and winter while in early spring (since the 440th day), the values of COP_{SWHP} for the three locations fall in the range of 5.5–6.5. This is due to the large variations in solar irradiance in autumn and winter and less variations in spring. The averaged values of COP_{SWHP} are 5.6, 5.6 and 5.4 in London, Aughton and Aberdeen, respectively. It is seen that the averaged value of COP_{SWHP} is much higher than that of COP_{ASHP} . This is attributed to the higher evaporation temperature of refrigerant in the water-to-refrigerant evaporator than that in the air-to-refrigerant evaporator.

Fig. 18 shows the daily variations of SPF_{HP} and SPF_{sys} over the heating season in London (blue), Aughton (orange) and Aberdeen (green). In all the three locations, the values of SPF_{SWHP} fall in the range of 4.0–6.5 and those of SPF_{ASHP} fall in the range of 3.5–4.5. In London, Aughton and Aberdeen, the seasonal SPF_{sys} are 4.4, 4.4 and 4.1 and the yearly SPF_{sys} are 4.9, 5.0 and 4.5. The yearly SPF_{sys} is in consistent with the value of solar extractable in the three locations. In autumn and spring, the values of SPF_{sys} are seen largely scattered and much higher

due to large variations in weather conditions. In addition, the fact that the heating demand for space heating decreases results in significant increase in the heating provided by direct SHW. Sometimes, the heating system in Aberdeen shows the highest SPF_{sys} . For example, SPF_{sys} until the 394th day in London, Aughton and Aberdeen are 3.9, 3.8 and 4.9, respectively.

5.3. Comparison of overall heating performance

Table 4 lists the overall operation performances of the heating system. The heat exchange with outdoor surroundings and the stored thermal energy in the TES tanks at the beginning and ending of the simulations are considered. In all the cases, the temperature for hot water and space heating is set to be the same. For each location, the heat provisions are similar because the heat demands are the same at different $T_{\rm HWS}^*$, but the provisions can vary slightly due to the influence of $T_{\rm HWS}^*$. Especially, when $T_{\rm HWS}^*$ is 40 °C, equal to the set hot water temperature, the temperature of hot water provided may be lower than the set hot water temperature after feed water enters TES tank 2. Therefore, heat provisions for hot water with a $T_{\rm HWS}^*$ of 40 °C is lower

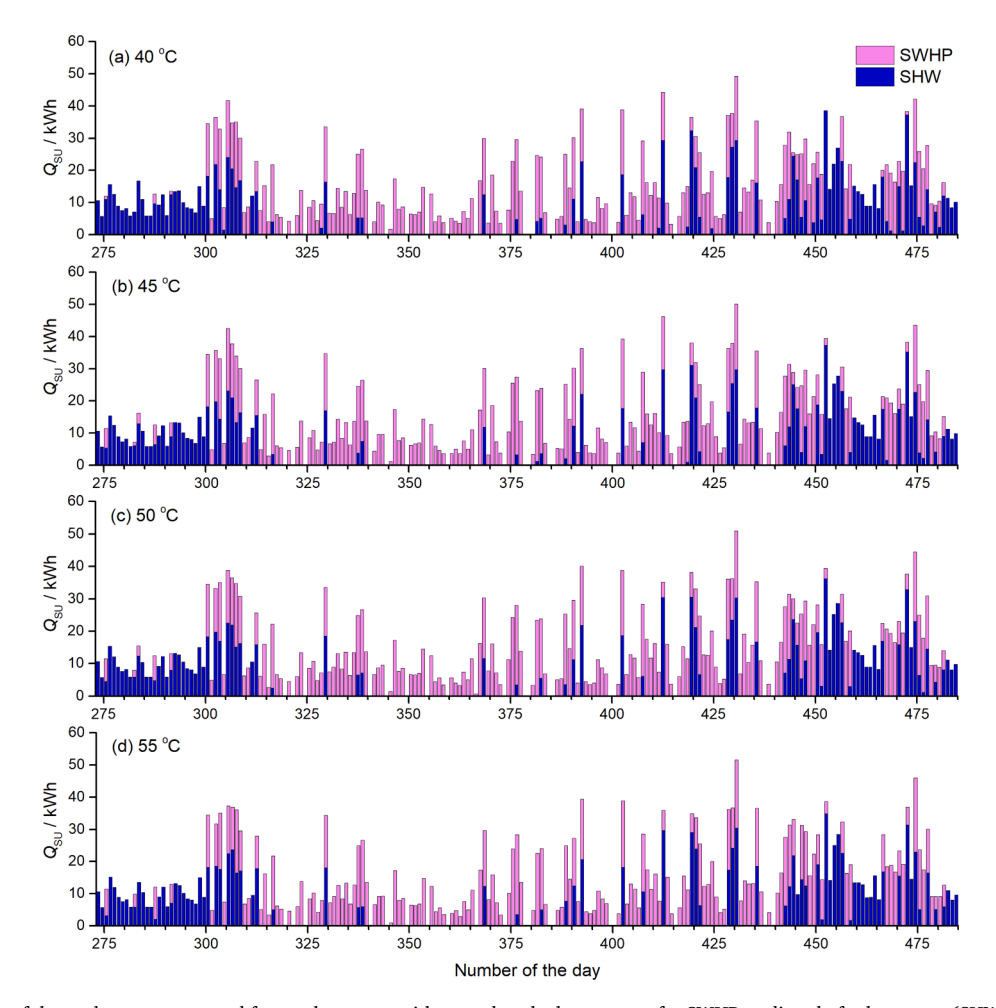


Fig. 9. Daily variations of thermal energy extracted from solar energy either used as the heat source for SWHP or directly for hot water (SHW) over a heating season for different T_{HWS}^* .

than those at other T_{HWS}^* in all the three locations.

The influence of $T_{\rm HWS}^*$ on heat provision for space heating is complex. $T_{\rm HWS}$ can influence the indoor air temperature and thus the heat provision period of the heating system. At a lower $T_{\rm HWS}^*$, the heat provision periods of both ASHP and SWHP are shorter and results in lower indoor air temperature within the temperature range for thermal comfort. Thus, the heat provision for SH is less. However, the indoor air temperature can influence the TES performance of the furniture inside the building that higher indoor air temperature brings more TES and requires less heat provision. The influence on total heat provisions is a combination of both effects. Generally, for the selected three locations, a $T_{\rm HWS}^*$ of 50 °C, the system achieves the highest heat provision for space heating.

Fig. 19 shows the variations of heat provision for space heating and hot water by SWHP, ASHP and direct SHW against $T_{\rm HWS}^*$ for heating systems operating in London (black), Aughton (red) and Aberdeen (blue). The lines are a guide for the eye. It can be seen that as $T_{\rm HWS}^*$ decreases, heat provision from HPs decreases and that from direct SHW increases. When $T_{\rm HWS}^*$ decreases from 55 °C to 50 °C, 45 °C and 40 °C, the contribution of SWHP decreases by 0.5 %, 2.6 % and 8.8 % in

London; by 1.8 %, 2.9 % and 6.6 % in Aughton; and by 1.6 %, 4.2 % and 8.0 % in Aberdeen. The heat provision from ASHP shows an inapparent decreasing trend. As $T_{\rm HWS}{}^{*}$ decreases from 55 °C to 50 °C, 45 °C and 40 °C, the contribution of ASHP decreases by 0.2 %, 0.5 % and 0.6 % in London; by 0.4 %, 0.2 % and 0.6 % in Aughton; and by 0.3 %, 0.1 % and 0.5 % in Aberdeen. At the same time, the contribution of direct SHW increases by 0.01 %, 1.0 % and 5.2 % in London; by 1.7 %, 1.2 % and 4.6 % in Aughton; and by 1.6 %, 2.8 % and 6.9 % in Aberdeen.

Fig. 20 displays the variations of electricity consumed by SWHP and ASHP and the total electricity consumed by the heating system against $T_{\rm HWS}{}^*$ for heating systems operating London (black), Aughton (red) and Aberdeen (blue). With the decrease of $T_{\rm HWS}{}^*$ from 55 °C to 50 °C, 45 °C and 40 °C, the electricity consumed by SWHP is decreased by 5.9 %, 13.1 % and 22.4 % in London; by 6.8 %, 12.1 % and 19.1 % in Aughton; and by 5.6 %, 13.8 % and 20.7 % in Aberdeen. The electricity consumed by ASHP is decreased by 5.7 %, 10.7 % and 14.6 % in London; by 5.9 %, 10.8 % and 15.0 % in Aughton; and by 3.9 %, 8.6 % and 12.3 % in Aberdeen.

Fig. 21 shows the variation of thermal energy extracted from solar energy and ambient air against T_{HWS}^* for heating systems operating in

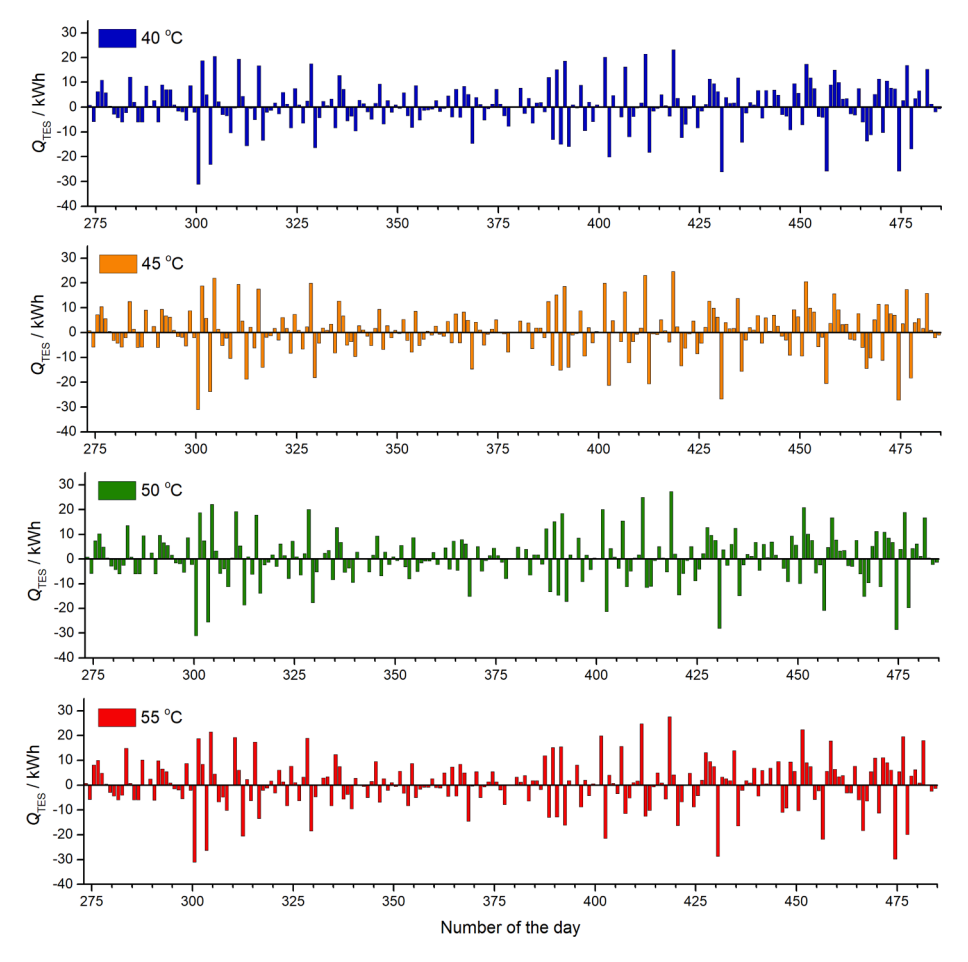


Fig. 10. Daily variations of Q_{TES} charged (positive) and discharged (negative) of tank 2 over a heating season for different T_{HWS}^* .

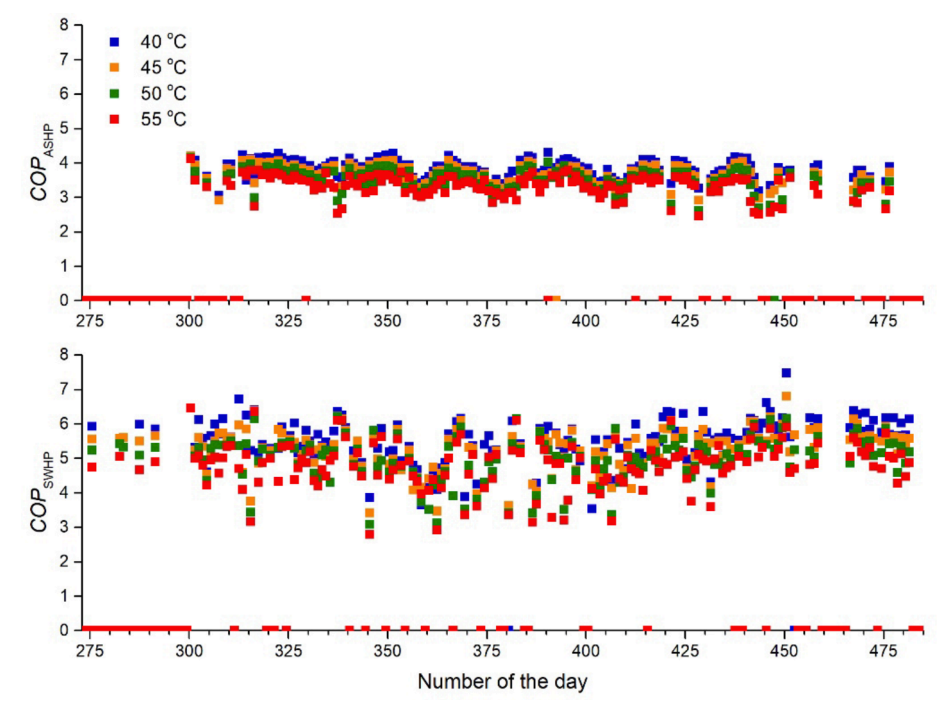


Fig. 11. Variations of daily averaged COP_{ASHP} and COP_{SWHP} over a heating season for different T_{HWS}^* .

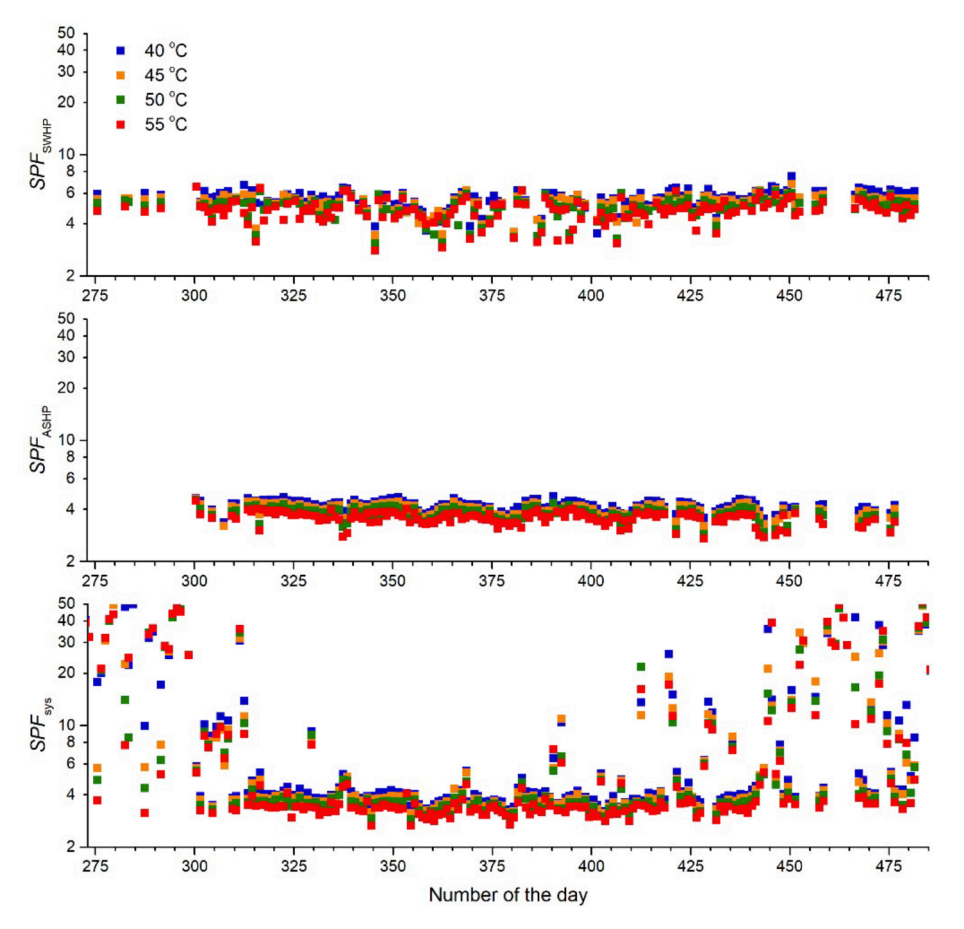


Fig. 12. Daily variations of SPF_{SWHP} , SPF_{ASHP} and SPF_{sys} over a heating season for different T_{HWS}^* .

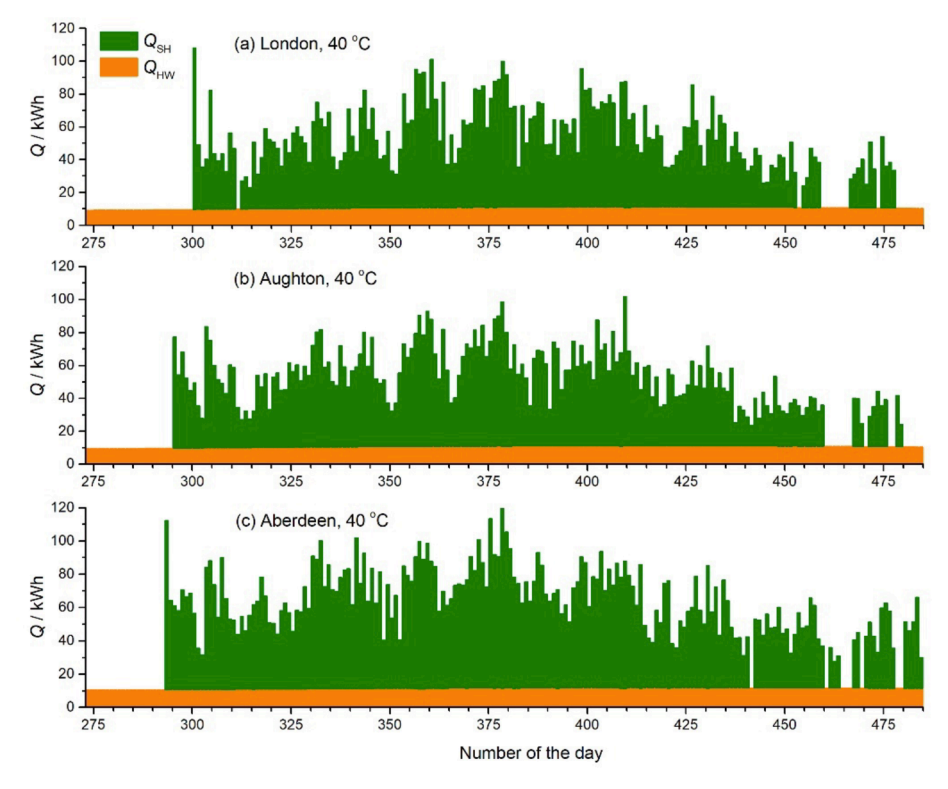


Fig. 13. Daily variations of heat provision for space heating and hot water over a heating season in London, Aughton and Aberdeen.

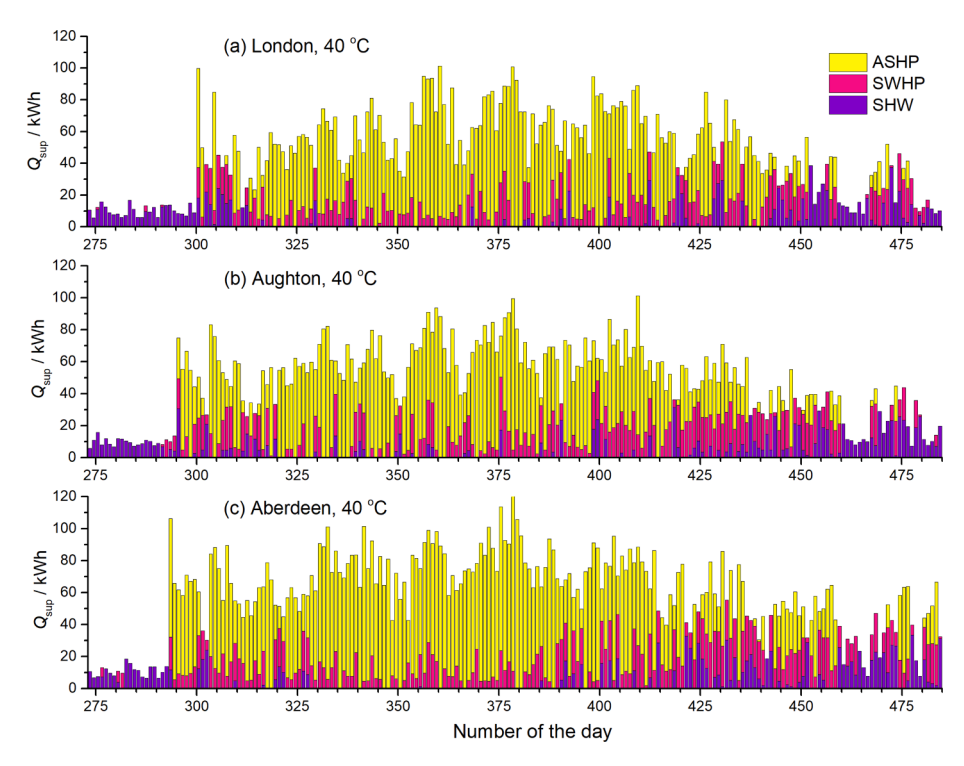


Fig. 14. Daily variations of heat provision for space heating and hot water by direct SHW, ASHP and SWHP over a heating season in London, Aughton and Aberdeen.

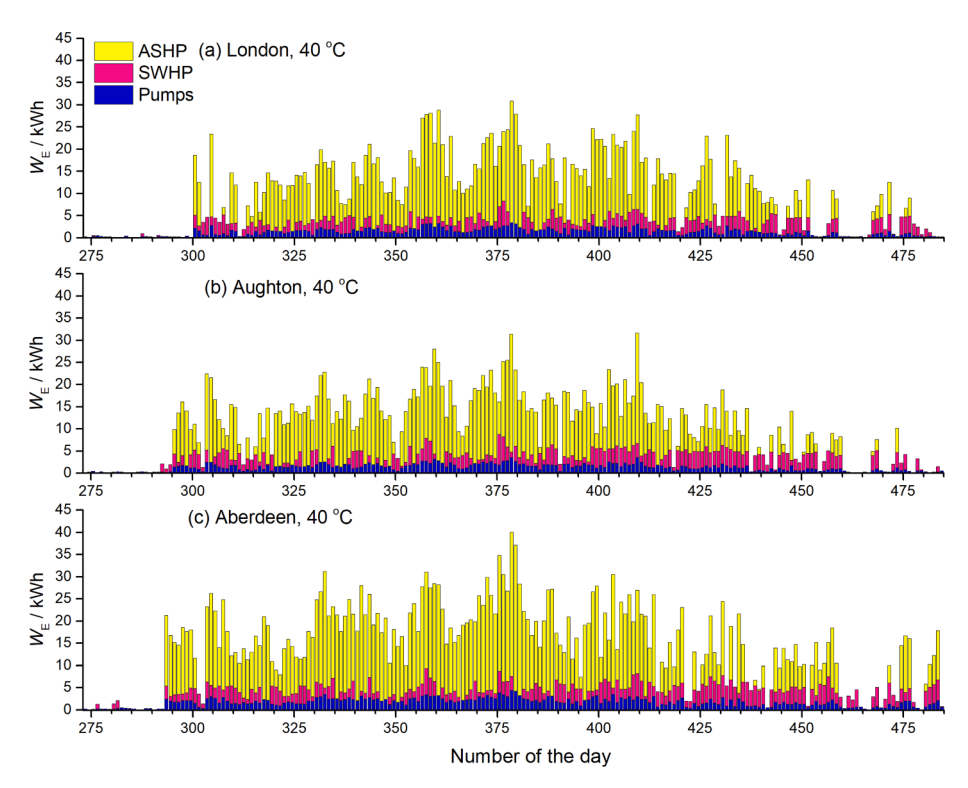


Fig. 15. Daily variations of electricity consumed by ASHP, SWHP and pumps over a heating season in London, Aughton and Aberdeen.

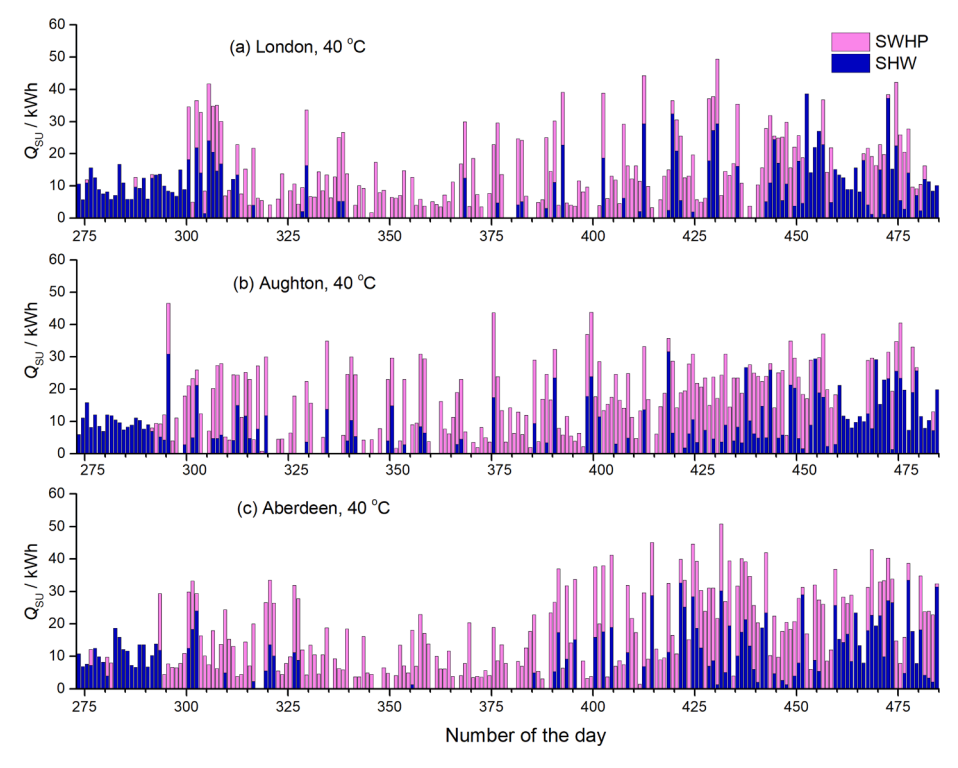


Fig. 16. Daily variations of thermal energy extracted from solar energy either used as the heat source for SWHP or directly for hot water (SHW) over a heating season in London, Aughton and Aberdeen.

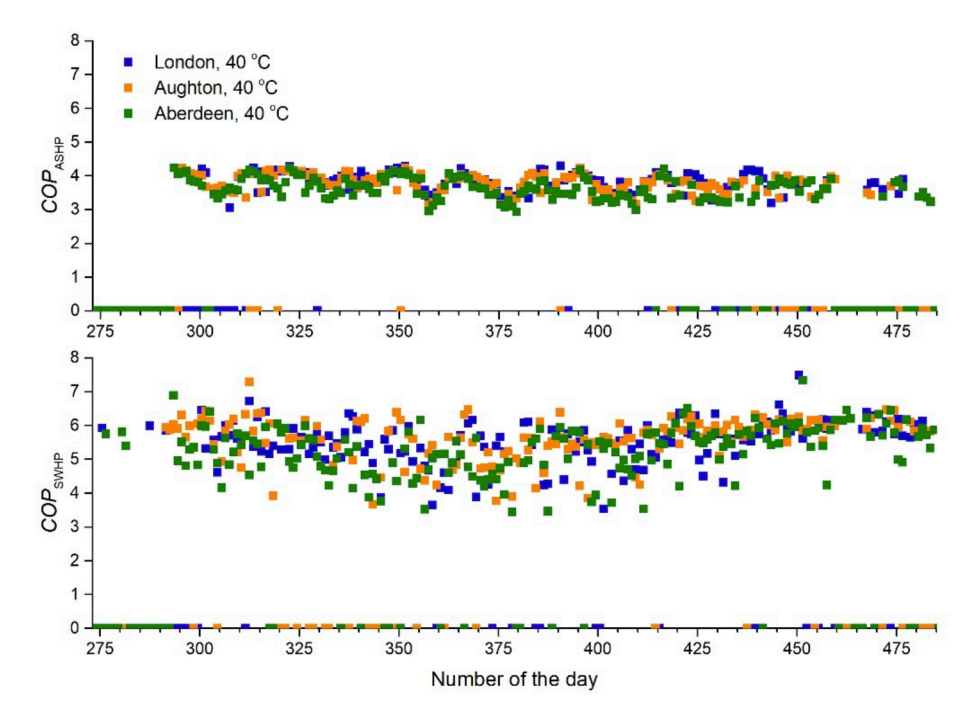


Fig. 17. Daily variations of averaged COP of the HPs over a heating season in London, Aughton and Aberdeen.

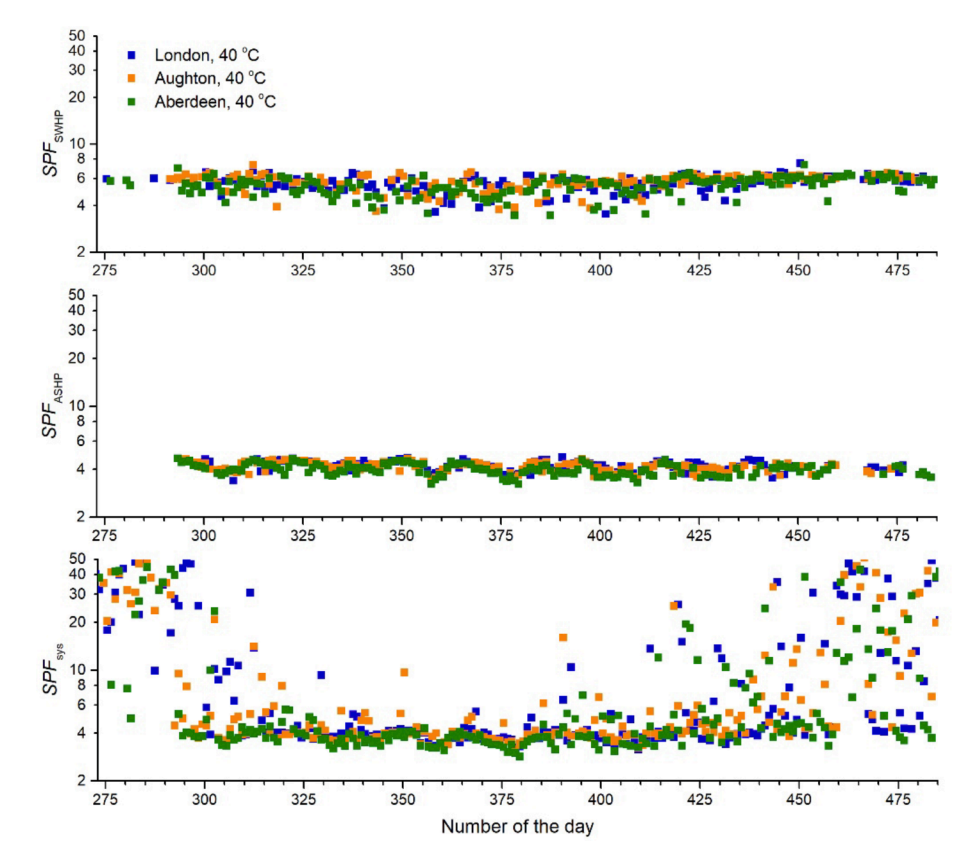


Fig. 18. Daily variations of SPF_{svs} and SPF_{HP} over a heating season in London, Aughton and Aberdeen.

London (black), Aughton (red) and Aberdeen (blue). With the decrease of $T_{\rm HWS}^*$ from 55 °C to 50 °C, 45 °C and 40 °C, thermal energy collection from ambient air increases by 1.9 %, 3.4 % and 4.9 % in London; by 1.8 %, 3.9 % and 5.2 % in Aughton; and by 1.2 %, 3.4 % and 4.4 % in Aberdeen. As $T_{\rm HWS}^*$ decreases from 55 °C to 50 °C, 45 °C and 40 °C, thermal energy collection from solar is increased by 0.4 %, 0.7 % and 1.2 % in London; by 0.7 %, 0.5 % and 1.2 % in Aughton; and by 0.7 %, 0.8 % and 1.6 % in Aberdeen.

Fig. 22 shows averaged *COP* of SWHP and ASHP with $T_{\rm HWS}^*$ for heating systems operating in London (black), Aughton (red) and Aberdeen (blue). With the decrease of $T_{\rm HWS}^*$ from 55 °C to 50 °C, 45 °C and 40 °C, the *COP* of SWHP increases by 4.2 %, 10.4 % and 16.7 % in London; by 4.0 %, 8.0 % and 12.0 % in Aughton; and by 2.1 %, 8.5 % and 14.9 % in Aberdeen. At the same time, the *COP* of ASHP increases by 6.1 %, 12.1 % and 15.2 % in London; by 6.3 %, 12.5 % and 18.8 % in Aughton; and by 3.1 %, 9.4 % and 12.5 % in Aberdeen.

Fig. 23 shows the variations of yearly and seasonally SF with $T_{\rm HWS}^*$ for heating systems operating in London (black), Aughton (red) and Aberdeen (blue). The SF in the heating season shows the similar variation trend with the heat provision for space heating. For the yearly SF, as $T_{\rm HWS}^*$ decreases from 55 °C to 50 °C, 45 °C and 40 °C, it increases from

39.5~% to $39.6~\%,\,39.8~\%$ and 39.9~% in London; from 42.0~% to $42.3~\%,\,42.2~\%$ and 42.5~% in Aughton; and from 36.6~% to $36.8~\%,\,36.8~\%$ and 37.1~% in Aberdeen.

Fig. 24 shows the variations of yearly and seasonally SPF_{HP} and SPF_{sys} with T_{HWS}^* in London (black), Aughton (red) and Aberdeen (blue). As T_{HWS}^* decreases from 55 °C to 50 °C, 45 °C and 40 °C, the SPF of SWHP increases by 6.3 %, 12.5 % and 18.8 % in London; by 6.0 %, 10.0 % and 16.0 % in Aughton; and by 4.3 %, 10.6 % and 17.0 % in Aberdeen. At the same time, the SPF of ASHP increases by 5.6 %, 11.1 % and 16.7 % in London; by 5.7 %, 11.4 % and 17.1 % in Aughton; and by 2.9 %, 8.6 % and 11.4 % in Aberdeen. When T_{HWS}^* decreases from 55 °C to 50 °C, 45 °C and 40 °C, the yearly SPF_{sys} increases by 4.8 %, 11.9 % and 16.7 % in London; by 7.1 %, 11.9 % and 19.1 % in Aughton; and by 5.1 %, 10.3 % and 15.4 % in Aberdeen. At the same time, the seasonally SPF_{sys} increases by 5.4 %, 13.5 % and 18.9 % in London; by 5.3 %, 10.5 % and 15.8 % in Aughton; and by 5.7 %, 11.4 % and 17.1 % in Aberdeen.

Low temperature heating helps to reduce electricity consumption, as shown in Fig. 25. For the heating system, with the decrease of $T_{\rm HWS}^*$ from 55 °C to 50 °C, 45 °C and 40 °C, the yearly electricity consumption decreases by 5.6 %, 10.5 % and 19.1 % in London; by 5.6 %, 10.4 % and 14.9 % in Aughton; by 4.4 %, 10.3 % and 13.3 % in Aberdeen. It is seen

 Table 4

 Overall performance of the heating system operating in London, Aughton and Aberdeen.

| System | Period | | London | | | | Aughton | | | | Aberdeen | | | |
|---------------------------------------|--------------|------------------|---------|---------|---------|---------|---------|---------|---------|---------|----------|---------|---------|---------|
| | | | 40 | 45 | 50 | 55 | 40 | 45 | 50 | 55 | 40 | 45 | 50 | 55 |
| Heat provision (kWh) | HW | Heating- | 2236.7 | 2237.8 | 2237.7 | 2237.7 | 2272 | 2273.0 | 2273.0 | 2272.6 | 2434.5 | 2439.9 | 2441.8 | 2440.7 |
| | | Non- | 1427.0 | 1427.2 | 1427.5 | 1427.2 | 1468.8 | 1468.9 | 1469.0 | 1468.9 | 1627.9 | 1628.3 | 1628.5 | 1628.4 |
| | | heating- | | | | | | | | | | | | |
| | SH | | 7512.0 | 7515.5 | 7527.9 | 7524.6 | 7675.4 | 7669.6 | 7676.9 | 7674.8 | 10052.4 | 10053.1 | 10053.5 | 10052.7 |
| | Total | | 11175.7 | 11180.4 | 11193.1 | 11189.5 | 11416.2 | 11411.5 | 11419.0 | 11416.2 | 14114.8 | 14121.2 | 14123.7 | 14121.8 |
| Heat provision | SWHP | | 2098.2 | 2239.3 | 2289.1 | 2299.6 | 2480.4 | 2579.1 | 2607.8 | 2656.6 | 2920.6 | 3039.3 | 3123.4 | 3173.0 |
| (kWh) | ASHP | | 6565.6 | 6568.1 | 6586.6 | 6602.1 | 6362.2 | 6382.0 | 6374.9 | 6397.4 | 8560.8 | 8593.0 | 8575.1 | 8600.6 |
| | Solar | Heating- | 1243.1 | 1195.9 | 1187.6 | 1194.1 | 1241.9 | 1171.0 | 1200.0 | 1158.5 | 1246.6 | 1217.8 | 1206.9 | 1180.4 |
| | | Non- | 1487.5 | 1427.1 | 1409.4 | 1402.6 | 1553.7 | 1533.4 | 1517.5 | 1514.9 | 1605.8 | 1525.9 | 1504.2 | 1488.9 |
| | | heating- | | | | | | | | | | | | |
| Electricity consumption (kWh) | SWHP | | 370.1 | 414.5 | 449.2 | 477.1 | 429.6 | 466.3 | 494.9 | 530.7 | 534.2 | 580.1 | 635.2 | 673.2 |
| | ASHP | | 1574.6 | 1646.0 | 1737.7 | 1843.3 | 1539.5 | 1616.1 | 1704.5 | 1810.9 | 2175.7 | 2268.3 | 2385.1 | 2481.7 |
| | Water | Heating- | 276.4 | 284.2 | 295.0 | 307.4 | 277.4 | 285.7 | 295.5 | 308.5 | 357.1 | 367.0 | 372.2 | 391.7 |
| | pumps | Non- heating- | 41.3 | 40.9 | 40.7 | 40.9 | 41.9 | 41.7 | 41.7 | 41.6 | 50.6 | 50.4 | 49.3 | 50.7 |
| | Total | · · | 2262.4 | 2385.7 | 2522.6 | 2668.8 | 2288.3 | 2409.8 | 2536.6 | 2691.7 | 3117.6 | 3265.7 | 3441.8 | 3597.3 |
| SPF_{HP} | SWHP | | 5.7 | 5.4 | 5.1 | 4.8 | 5.8 | 5.5 | 5.3 | 5 | 5.5 | 5.2 | 4.9 | 4.7 |
| | ASHP | | 4.2 | 4.0 | 3.8 | 3.6 | 4.1 | 3.9 | 3.7 | 3.5 | 3.9 | 3.8 | 3.6 | 3.5 |
| Heat provision period (hour) | SWHP | | 301.63 | 315.89 | 327.25 | 333.25 | 351.38 | 364.13 | 371.63 | 385.13 | 411.13 | 420.89 | 415.13 | 452.5 |
| | ASHP | | 743.00 | 743.75 | 746.38 | 759.00 | 725.13 | 727.75 | 727.50 | 740.38 | 997 | 1000.13 | 899.25 | 1006.3 |
| Electricity consumption per kWh heat | SWHP | | 0.18 | 0.19 | 0.20 | 0.21 | 0.17 | 0.18 | 0.19 | 0.20 | 0.18 | 0.19 | 0.20 | 0.21 |
| provision (kWh) | ASHP | | 0.24 | 0.25 | 0.26 | 0.28 | 0.24 | 0.25 | 0.27 | 0.28 | 0.25 | 0.26 | 0.28 | 0.29 |
| COP_{ave} | SWHP | | 5.6 | 5.3 | 5.0 | 4.8 | 5.6 | 5.4 | 5.2 | 5.0 | 5.4 | 5.1 | 4.8 | 4.7 |
| | ASHP | | 3.8 | 3.7 | 3.5 | 3.3 | 3.8 | 3.6 | 3.4 | 3.2 | 3.6 | 3.5 | 3.3 | 3.2 |
| Solar thermal energy (kWh) | To SWHP | | 1728.1 | 1824.8 | 1839.9 | 1822.5 | 2050.8 | 2112.7 | 2113.0 | 2125.9 | 2386.4 | 2459.3 | 2488.1 | 2499.8 |
| | To end use | Heating- | 1243.1 | 1195.9 | 1187.6 | 1194.1 | 1241.9 | 1171.0 | 1200.2 | 1158.5 | 1246.6 | 1217.8 | 1206.9 | 1180.4 |
| | | Non- | 1487.5 | 1427.1 | 1409.4 | 1402.6 | 1553.7 | 1533.4 | 1517.5 | 1514.9 | 1605.8 | 1525.9 | 1504.2 | 1488.9 |
| | | heating- | | | | | | | | | | | | |
| | Total | _ | 4739.8 | 4720.9 | 4706.7 | 4686.0 | 5131.0 | 5095.5 | 5103.9 | 5070.2 | 5515.9 | 5471.6 | 5464.3 | 5427.6 |
| Thermal energy from ambient air (kWh) |) | | 4991.0 | 4922.0 | 4848.9 | 4758.7 | 4822.7 | 4765.9 | 4670.4 | 4586.5 | 6385.1 | 6324.7 | 6190.0 | 6118.9 |
| SF | Heating seas | son | 30.5 % | 31.0 % | 31.0 % | 30.9 % | 33.1 % | 33.0 % | 33.3 % | 33.0 % | 29.1 % | 29.4 % | 29.6 % | 29.5 % |
| | Yearly | | 39.9 % | 39.8 % | 39.6 % | 39.5 % | 42.5 % | 42.2 % | 42.3 % | 42.0 % | 37.1 % | 36.8 % | 36.8 % | 36.6 % |
| SPF _{sys} | Heating seas | son | 4.4 | 4.2 | 3.9 | 3.7 | 4.4 | 4.2 | 4.0 | 3.8 | 4.1 | 3.9 | 3.7 | 3.5 |
| . · | Yearly | | 4.9 | 4.7 | 4.4 | 4.2 | 5.0 | 4.7 | 4.5 | 4.2 | 4.5 | 4.3 | 4.1 | 3.9 |

Note: Heating-: Heating season; Non-heating-: Non-heating season.

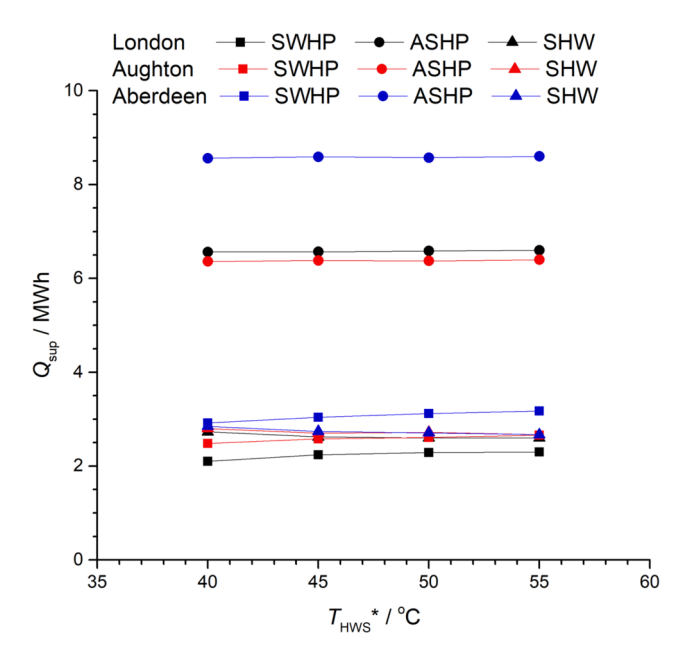


Fig. 19. Variations of heat provision for space heating and hot water by SWHP, ASHP and direct SHW against $T_{\rm HWS}{}^*$ for heating systems operating in London, Aughton and Aberdeen.

that at a higher water supply temperature, the electricity savings for three locations are generally the same; at a lower water supply temperature, more electricity savings can be achieved in location at lower latitude.

6. Economic analyses

Economic analyses are conducted for the heating system with different $T_{\rm HWS}{}^*$ against electric water heater in London, Aughton and Aberdeen.

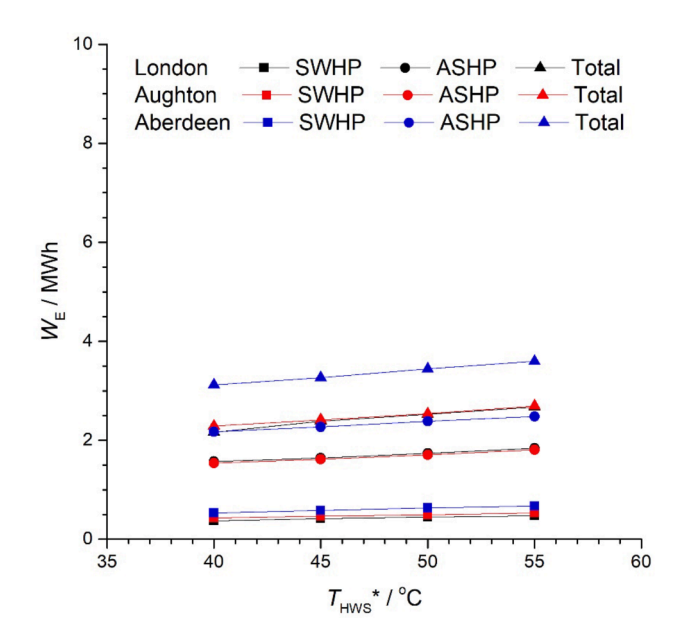


Fig. 20. Variations of electricity consumed by SWHP and ASHP and the total electricity consumed by the heating system against $T_{\rm HWS}{}^*$ for heating systems operating London, Aughton and Aberdeen.

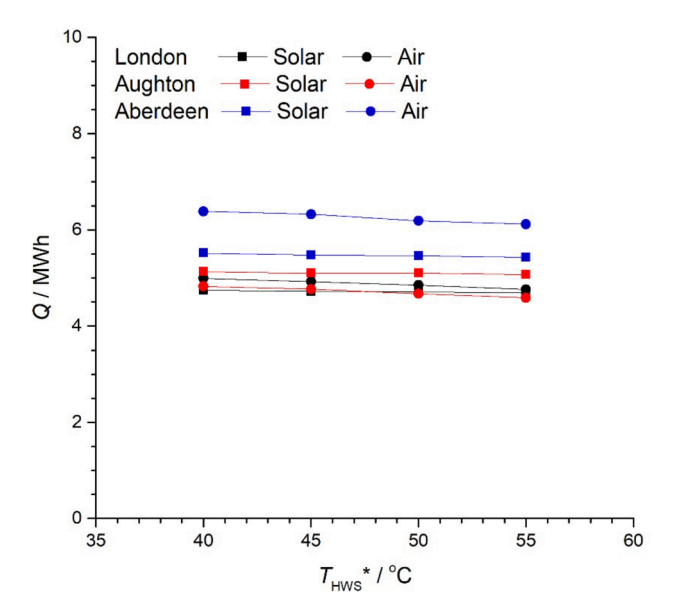


Fig. 21. Variation of thermal energy (Q) extracted from solar energy and ambient air against $T_{\rm HWS}{}^*$ for heating systems operating in London, Aughton and Aberdeen.

 W_{tot} is the total electricity consumed by the heating systems calculated by Eq. (8):

$$W_{tot} = (Q_{SH} + Q_{HW})/\eta \tag{8}$$

where η is the heater efficiency.

 $P_{\rm pb}$ is the payback period against electric water heater, calculated by Eq. (9):

$$P_{pb} = C_i / C_{spy} \tag{9}$$

where C_i is the difference of the initial cost and $C_{\rm spy}$ is the cost saving

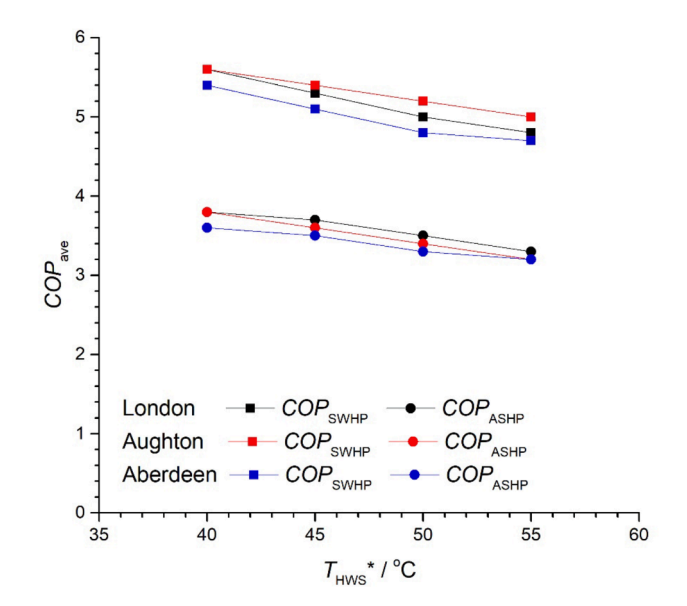


Fig. 22. Averaged COP of SWHP and ASHP with $T_{\rm HWS}{}^*$ for heating systems operating in London, Aughton and Aberdeen.

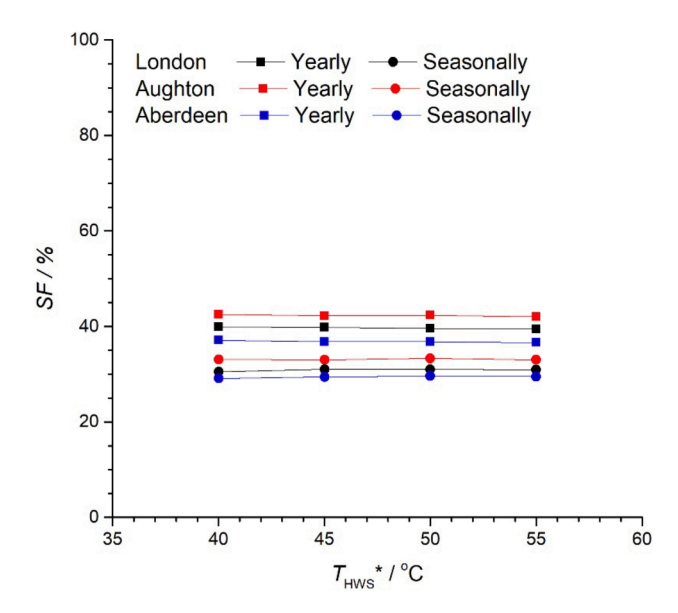


Fig. 23. Variations of yearly and seasonally SF with $T_{\rm HWS}^*$ for heating systems operating in London, Aughton and Aberdeen.

per year, obtained by Eq.(10) and Eq.(11).

$$C_i = C_{i0} - C_{ieh} (10)$$

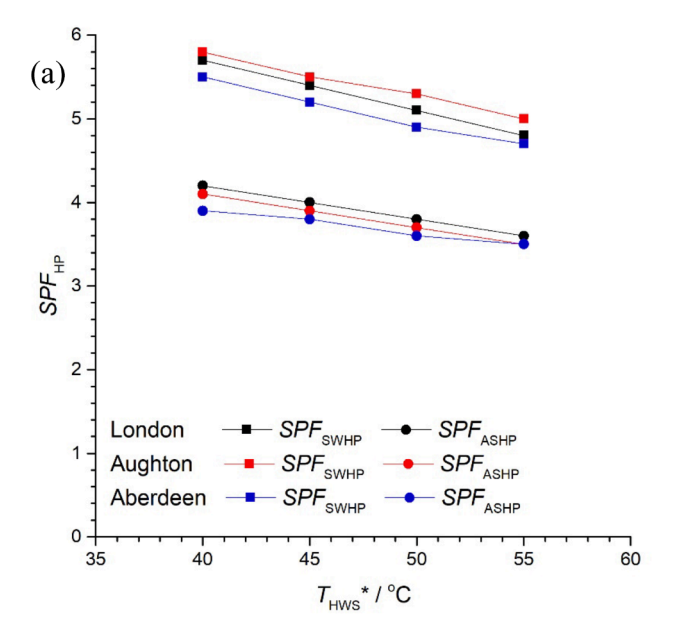
$$C_{spv} = C_{o0} - C_{oeh} \tag{11}$$

where C_{i0} and C_{o0} are the initial and operation costs of the heating system, C_{ieh} and C_{oeh} are the initial and operation costs of the electric water heater, respectively.

The efficiency of the electric water heater is taken from (Li and Yang, 2009) to be 0.95. The electric water heater has a domestic TES tank of 300 L. The heat provision of electric water heater is set to be the average heat provision of the heating system at that location. Energy prices are seen significant increase in the past year. The electricity price is taken from E.On Energy (a UK energy suppler) to be £212.2 per MWh in April 2021, £293.2 per MWh in December 2021, £343.9 per MWh in January 2022 and £384.6 per MWh in April 2022 (E.ON Energy).

The price of the heating systems is assumed based on quote from an online market. The flat plate solar collector costs around £30 per $\rm m^2$, TES tank costs £290 per 100 L, and a pump of 15-m head and 15 L/min flow rate costs around £10 (https://www.made-in-china.com). The heating systems used in the all the three locations have a capacity of 8 kW. Installation of the heating system is assumed to be 6 h with an engineer fee of £80 per hour (Costs, 2021). The economic analyses for different $T_{\rm HWS}$ * for 2021 and 2022 at three locations are displayed in tables 5 and 6.

The payback periods decrease as $T_{\rm HWS}{}^*$ decreases. With the decrease of $T_{\rm HWS}{}^*$ from 55 °C to 50 °C, 45 °C and 40 °C, in 2022, the payback periods decrease by 2.0 %, 3.0 % and 5.9 % in London; by 1.0 %, 2.0 % and 4.1 % in Aughton; by 1.2 %, 2.5 % and 3.7 % in Aberdeen. Among the three selected locations, Aberdeen has the highest heat demand, 26.3 % higher than that in London, and the lowest payback periods,



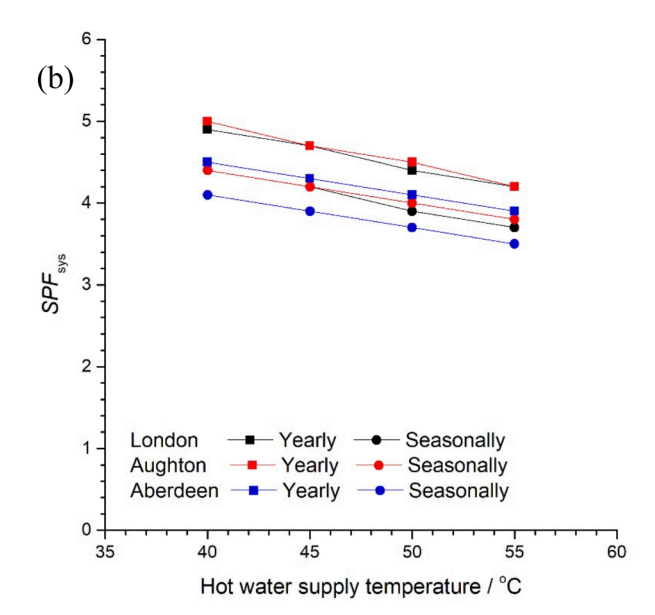


Fig. 24. Variations of yearly and seasonally (a) $SPF_{\rm HP}$ and (b) $SPF_{\rm sys}$ with $T_{\rm HWS}^*$ in London, Aughton and Aberdeen.

around 19 % lower than those in London.

Fig. 26 shows the payback period at $T_{\rm HWS}^*$ of 40 °C, 45 °C, 50 °C and 55 °C against electricity price in London, Aughton and Aberdeen. In the past one year, the electricity price is seen sharp increase from £212.2 per MWh (April 2021) to £293.2 (December 2021), £343.9 (January 2022) and £384.6 per MWh (April 2022). Compared to the payback period in April 2021, the payback periods are significantly reduced by around

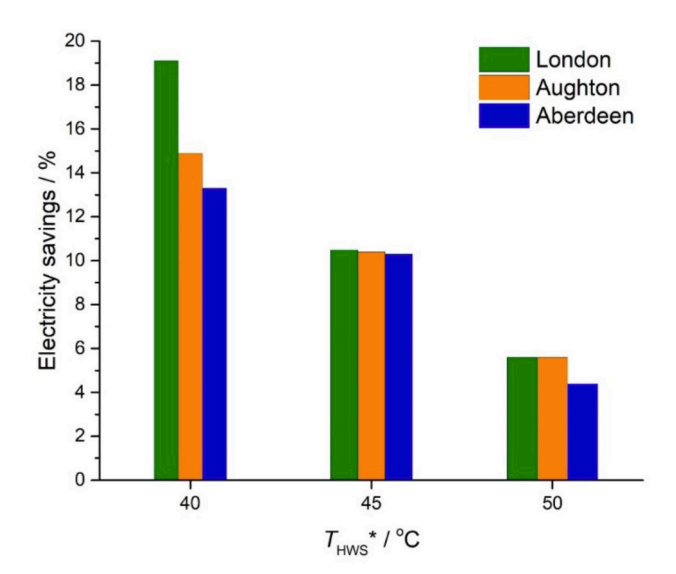


Fig. 25. Electricity savings at $T_{\rm HWS}^*$ of 40 °C, 45 °C and 50 °C compared with electricity consumption at $T_{\rm HWS}^*$ of 55 °C.

27.7 %, 38 % and 45 %, respectively. In this situation, the differences among the payback periods with different $T_{\rm HWS}^*$ are reduced. Note that the current economic analysis is based on component prices from an online international market and the labour price in 2021. These prices are significantly higher in 2022 and result in some variation in payback period.

7. Conclusions

TRNSYS has been used to simulate the low temperature operation performance of dual-source IX-SAASHPs under the weather conditions in London, Aughton and Aberdeen in the UK, respectively. Based on energy and economic analyses, the conclusions below can be obtained:

- (1) Low temperature heating can significantly reduce electricity consumption. For the heating system, with the decrease of the set hot-water-supply temperature from 55 °C to 40 °C, the yearly electricity consumption decreases by 19.1 % in London, 14.9 % in Aughton, and 13.3 % in Aberdeen, respectively.
- (2) Low temperature heating increases thermal energy collection from both solar energy and ambient air, and hence *COP* largely increases. With the decrease of the set hot-water-supply temperature from 55 °C to 40 °C, the *COP* of SWHP increases from 4.8 to 5.6 in London, from 5.0 to 5.6 in Aughton; and from 4.7 to 5.4 in Aberdeen, respectively, while the *COP* of ASHP increases from 3.3 to 3.8 in London; from 3.2 to 3.8 in Aughton; and from 3.2 to 3.6 in Aberdeen, respectively.
- (3) Low temperature heating benefits to decrease heat provision from ASHP and SWHP and to increase the heat provision from direct SHW, resulting in much better system efficiency. When the set hot-water-supply temperature decreases from 55 °C to 40 °C, the yearly *SPF*_{sys} increases from 4.2 to 4.9 in London; from 4.2 to 5.0 in Aughton; and from 3.9 to 4.5 in Aberdeen, respectively.
- (4) At the set hot-water-supply temperature of 40 °C, the heat provided by ASHP is about three times of that by SWHP and about six times of that by direct SHW, and the electricity consumed by ASHP is about four times of that by SWHP and about five times of that by pumps in the three locations.
- (5) SF appears to be negligibly influenced by latitude and set hotwater-supply-temperature. For different set hot-water-supply-temperature, SF is 40 % in London, 42 % in Aughton, and 37 % in Aberdeen.

Results of economic analysis for dual-source IX-SAASHP heating systems in London (April 2021).

| • | | | , , | | | | | | | | | | | | |
|---------------------------------|------------|-----------------------|----------|--------|--------|--------|--------|---------|--------|--------|--------|----------|--------|--------|--------|
| | Electric w | Electric water heater | | London | | | | Aughton | | | | Aberdeen | | | |
| | London | Aughton | Aberdeen | 40 | 45 | 20 | 55 | 40 | 45 | 20 | 22 | 40 | 45 | 20 | 55 |
| eat provision per year, MWh | 11.18 | 11.42 | 14.12 | 11.18 | 11.18 | 11.19 | 11.19 | 11.42 | 11.41 | 11.42 | 11.42 | 14.11 | 14.12 | 14.12 | 14.12 |
| ficiency/performance | 0.95 | 0.95 | 0.95 | 4.9 | 4.7 | 4.4 | 4.2 | 2 | 4.7 | 4.5 | 4.2 | 4.5 | 4.3 | 4.1 | 3.9 |
| lergy consumption per year, MWh | 11.77 | 12 | 14.86 | 2.16 | 2.39 | 2.52 | 2.67 | 2.29 | 2.41 | 2.54 | 2.69 | 3.12 | 3.23 | 3.44 | 3.60 |
| itial cost, £ collector | 0 | 0 | 0 | 540 | 540 | 540 | 540 | 540 | 540 | 540 | 540 | 540 | 540 | 540 | 540 |
| tanks | 870 | 870 | 870 | 2320 | 2320 | 2320 | 2320 | 2320 | 2320 | 2320 | 2320 | 2320 | 2320 | 2320 | 2320 |
| Heater/HP | 09 | 09 | 09 | 1085 | 1085 | 1085 | 1085 | 1085 | 1085 | 1085 | 1085 | 1085 | 1085 | 1085 | 1085 |
| sdund | 0 | 0 | 0 | 30 | 30 | 30 | 30 | 30 | 30 | 30 | 30 | 30 | 30 | 30 | 30 |
| Installation | 0 | 0 | 0 | 480 | 480 | 480 | 480 | 480 | 480 | 480 | 480 | 480 | 480 | 480 | 480 |
| total | 930 | 930 | 930 | 4455 | 4455 | 4455 | 4455 | 4455 | 4455 | 4455 | 4455 | 4455 | 4455 | 4455 | 4455 |
| peration cost, £ | 2497.2 | 2546.0 | 3152.8 | 458.3 | 507.1 | 534.7 | 566.5 | 485.9 | 511.3 | 538.9 | 570.7 | 662.0 | 685.3 | 729.9 | 763.8 |
| ost saving per year, £ | ı | ı | 1 | 2039.0 | 1990.2 | 1962.6 | 1930.7 | 2060.2 | 2034.7 | 2007.1 | 1975.3 | 2490.9 | 2467.5 | 2423.0 | 2389.0 |
| yback period, year | ı | ı | ı | 1.73 | 1.77 | 1.80 | 1.83 | 1.71 | 1.73 | 1.76 | 1.78 | 1.42 | 1.43 | 1.45 | 1.48 |

Results of economic analysis for dual-source IX-SAASHP heating systems in London (April 2022).

| | Electric wa | Electric water heater | | London | | | | Aughton | | | | Aberdeen | | | |
|----------------------------------|-------------|-----------------------|----------|--------|--------|--------|--------|---------|--------|--------|--------|----------|--------|--------|--------|
| | London | London Aughton | Aberdeen | 40 | 45 | 20 | 22 | 40 | 45 | 20 | 22 | 40 | 45 | 20 | 22 |
| Heat provision per year, MWh | 11.18 | 11.42 | 14.12 | 11.18 | 11.18 | 11.19 | 11.19 | 11.42 | 11.41 | 11.42 | 11.42 | 14.11 | 14.12 | 14.12 | 14.12 |
| Efficiency/performance | 0.95 | 0.95 | 0.95 | 4.9 | 4.7 | 4.4 | 4.2 | 2 | 4.7 | 4.5 | 4.2 | 4.5 | 4.3 | 4.1 | 3.9 |
| Energy consumption per year, MWh | 11.77 | 12 | 14.86 | 2.16 | 2.39 | 2.52 | 2.67 | 2.29 | 2.41 | 2.54 | 2.69 | 3.12 | 3.23 | 3.44 | 3.60 |
| Initial cost, £ collector | 0 | 0 | 0 | 540 | 540 | 540 | 540 | 540 | 540 | 540 | 540 | 540 | 540 | 540 | 540 |
| tanks | 870 | 870 | 870 | 2320 | 2320 | 2320 | 2320 | 2320 | 2320 | 2320 | 2320 | 2320 | 2320 | 2320 | 2320 |
| Heater/HP | 09 | 09 | 09 | 1085 | 1085 | 1085 | 1085 | 1085 | 1085 | 1085 | 1085 | 1085 | 1085 | 1085 | 1085 |
| sdumd | 0 | 0 | 0 | 30 | 30 | 30 | 30 | 30 | 30 | 30 | 30 | 30 | 30 | 30 | 30 |
| Installation | 0 | 0 | 0 | 480 | 480 | 480 | 480 | 480 | 480 | 480 | 480 | 480 | 480 | 480 | 480 |
| total | 930 | 930 | 930 | 4455 | 4455 | 4455 | 4455 | 4455 | 4455 | 4455 | 4455 | 4455 | 4455 | 4455 | 4455 |
| Operation cost, £ | 4526.7 | 4615.2 | 5715.2 | 830.7 | 919.2 | 969.1 | 1026.9 | 880.7 | 926.9 | 6.976 | 1034.6 | 1200.0 | 1242.3 | 1323.0 | 1384.6 |
| Cost saving per year, £ | I | ı | ı | 3696.0 | 3607.5 | 3557.6 | 3499.9 | 3734.5 | 3688.3 | 3638.3 | 3580.6 | 4515.2 | 4472.9 | 4392.1 | 4330.6 |
| Payback period, year | I | ı | I | 0.95 | 86.0 | 0.99 | 1.01 | 0.94 | 96.0 | 0.97 | 0.98 | 0.78 | 0.79 | 8.0 | 0.81 |

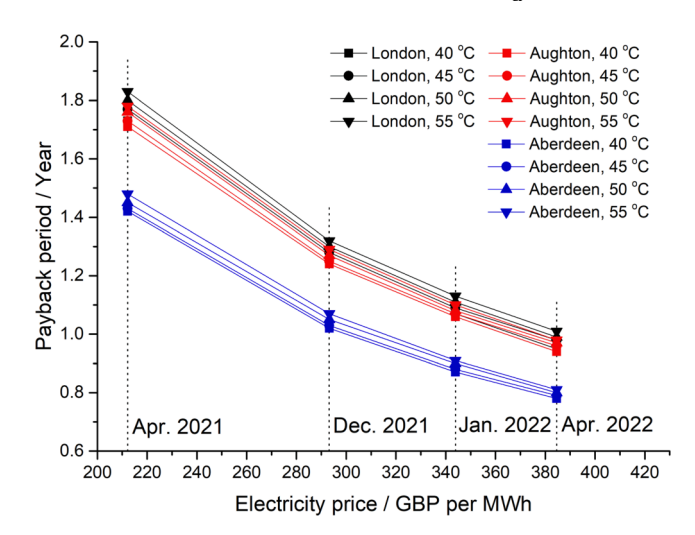


Fig. 26. variations of payback period at T_{HWS}^* of 40 °C, 45 °C, 50 °C and 55 °C with electricity price. The solid line is a guide for the eye.

(6) The payback periods slightly decrease as the set hot-water-supply temperature decreases. With the decrease of the set hot-water-supply-temperature from 55 °C to 40 °C, for the electricity price in April 2022, the payback periods decrease from 1.01 year to 0.95 year in London, from 0.98 year to 0.94 year in Aughton, and from 0.81 year to 0.78 year in Aberdeen.

Declaration of Competing Interest

The authors declare that they have no known competing financial interests or personal relationships that could have appeared to influence the work reported in this paper.

Acknowledgements

The authors gratefully acknowledge the financial supports from the Joint PhD Studentship of China Scholarship Council (CSC) and Queen Mary University of London (201808060459) and the Wuhan Applied Foundational Frontier Project (No. 2020010601012172).

References

Charted Institute of Plumbing and Heating Engineering, https://www.ciphe.org.uk/consumer/safe-water-campaign/hot-water-scalds/, [accessed on January 20th, 2021].

Chaturvedi, S.K., Gagrani, V.D., Abdel-Salam, T.M., 2014. Solar-assisted heat pump – A sustainable system for low-temperature water heating applications. Energy Convers Manage 77, 550–557.

Committee on Climate Change, The Sixth Carbon Budget – The UK's Path to Net Zero, 2020, https://www.theccc.org.uk/publication/sixth-carbon-budget/.

Plumber Costs: 2021 Call Out Charges & Hourly Prices UK, https://tradesmencosts.co. uk/plumbers/, [accessed on January 20th, 2022].

Dott, R., Haller, M.Y., Ruschenburg, J., Ochs, F., Bony, J., 2013. The Reference Framework for System Simulations of the IEA SHC Task 44 / HPP Annex 38—Part B: Buildings and Space Heat Load, A technical report of subtask C—Report C1 Part B. International Energy Agency.

E.ON Energy, https://www.eonenergy.com/for-your-home/products-and-services/best-deal-for-you/quote, [accessed on January 20th, 2022].
Fraga, C., Hollmuller, P., Mermoud, F., Lachal, B., 2017. Solar assisted heat pump system

Fraga, C., Hollmuller, P., Mermoud, F., Lachal, B., 2017. Solar assisted heat pump system for multifamily buildings: Towards a seasonal performance factor of 5? Numerical sensitivity analysis based on a monitored case study. Solar Energy 146, 543–564.

Golmohamadi, H., Larsen, K.G., 2022. Economic heat control of mixing loop for residential buildings supplied by low-temperature district heating. J Build Eng 46, 103286. https://doi.org/10.1016/j.jobe.2021.103286.

103286. https://doi.org/10.1016/j.jobe.2021.103286.

Hesaraki, A., Ploskic, A., Holmberg, S., 2015. Integrating low-temperature heating systems into energy efficient buildings. Energy Procedia 78, 3043–3048.

https://www.made-in-china.com, [accessed on January 20th, 2022].

International Energy Agency, Annex TS2 Implementation of Low-Temperature District Heating Systems, https://www.iea-dhc.org/securedl/sdl-eyJ0eXAiOiJKV1QiLCJhbGciOiJIUzI1NiJ9.

eyJpYXQiOjE2NTQ4NjQxNDEsImV4cCI6MTY1NDk1NDE0MCwidXNlciI6MC

- wiZ3JvdXBzIjpbMCwtMV0sImZpbGUiOiJmaWxlYWRtaW5cL2RvY3VtZW50c1wvQ W5uZXhfVFMyXC9JRUFfREhDX0FubmV4X1RTMI9Uc mFuc2l0aW9uX3RvX2xvd190ZW1wZXJhdHVyZV9ESC5wZGYiLCJwYWdlIjo1MjB9. tRalfkPPdZp9GulZNRGnTSmZi6YnUvCmdKxFSFFCiXs/IEA_DHC_Annex_TS2_Transition_to_low_temperature_DH.pdf.
- Kilkis, B., 2021. An exergy-based minimum carbon footprint model for optimum equipment oversizing and temperature peaking in low-temperature district heating systems. Energy 236, 121339. https://doi.org/10.1016/j.energy.2021.121339.
- Kong, X., Sun, P., Li, Y., Jiang, K., Dong, S., 2018. Experimental studies of a variable capacity direct-expansion solar-assisted heat pump water heater in autumn and winter conditions. Solar Energy 170, 352–357.
- Kong, X., Zhang, M., Yang, Y., Li, Y., Wang, D., 2020. Comparative experimental analysis of direct-expansion solar-assisted heat pump water heaters using R134a and R290. Solar Energy 203, 187–196.
- Li, H., Yang, H., 2009. Potential application of solar thermal systems for hot water production in Hong Kong, Appl Energy 86 (2), 175–180.
- Ma, J., Fung, A.S., Brands, M., Juan, N., Mohammad Abul Moyeed, O., 2020. Performance analysis of indirect-expansion solar assisted heat pump using CO2 as refrigerant for space heating in cold climate. Solar Energy 208, 195–205.
- Nord, N., Løve Nielsen, E.K., Kauko, H., Tereshchenko, T., 2018. Challenges and potentials for low-temperature district heating implementation in Norway. Energy 151, 889–902.
- Quirosa, G., Torres, M., Soltero, V.M., Chacartegui, R., 2022. Energetic and economic analysis of decoupled strategy for heating and cooling production with CO2 booster heat pumps for ultra-low temperature district network. J Build Eng 45, 103538. https://doi.org/10.1016/j.jobe.2021.103538.
- Ran, S., Li, X., Xu, W., Wang, B., 2020. A solar-air hybrid source heat pump for space heating and domestic hot water. Solar Energy 199, 347–359.

- Reiners, T., Gross, M., Altieri, L., Wagner, H.-J., Bertsch, V., 2021. Heat pump efficiency in fifth generation ultra-low temperature district heating networks using a wastewater heat source. Energy 236, 121318. https://doi.org/10.1016/j. energy.2021.121318.
- Ruschenburg, J., Herkel, S., Henning, H.M., 2013. A statistical analysis on marketavailable solar thermal heat pump systems. Solar Energy 95, 79–89.
- Sarbu, I., Sebarchievici, C., 2015. A study of the performances of low-temperature heating systems. Energy Efficiency 8 (3), 609–627.
- Schmidt, D., Lygnerud, K., Werner, S., Geyer, R., Schrammel, H., Østergaard, D.S., Gudmundsson, O., 2021. Successful implementation of low temperature district heating case studies. Energy Reports 7, 483–490.
- Xian, T., Wu, J., Zhang, X., 2020. Study on the operating characteristics of a solar heat pump water heater based on data fusion. Solar Energy 212, 113–124.
- Yang, L.W., Xu, R.J., Hua, N., Xia, Y.u., Zhou, W.B., Yang, T., Belyayev, Y., Wang, H.S., 2021. Belyayev Ye, Wang HS, Review of the advances in solar-assisted air source heat pumps for the domestic sector, Energy Convers. Manage 247, 114710. https://doi.org/10.1016/j.enconman.2021.114710.
- Yang, L.W., Hua, N., Pu, J.H., Xia, Y., Zhou, W.B., Xu, R.J., Yang, T., Belyayev, Y., Wang, H.S., 2022. Belyayev Ye, Wang HS, Analysis of operation performance of three indirect expansion solar assisted air source heat pumps for domestic heating, Energy Convers. Manage 252, 115061. https://doi.org/10.1016/j.enconman.2021.115061.
- Yang, X., Li, H., Svendsen, S., 2016. Energy, economy and exergy evaluations of the solutions for supplying domestic hot water from low-temperature district heating in Denmark. Energy Convers Manage 122, 142–152.
- Zhu, T., Ommen, T., Meesenburg, W., Thorsen, J.E., Elmegaard, B., 2021. Steady state behavior of a booster heat pump for hot water supply in ultra-low temperature district heating network. Energy 237, 121528. https://doi.org/10.1016/j. energy.2021.121528.